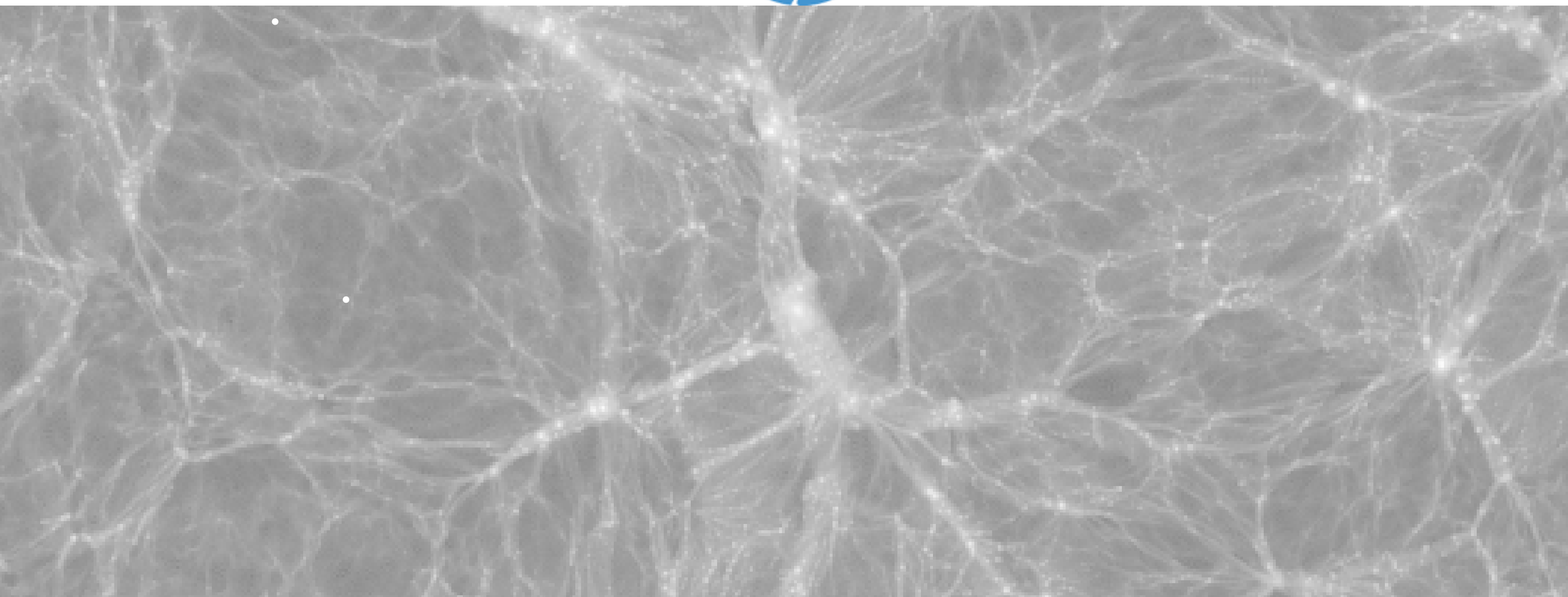

GALAXY INTRINSIC ALIGNMENT POWER SPECTRUM IN ILLUSTRIS-TNG

Jingjing Shi /史晶晶 (with Masahiro Takada, Toshiki Kurita, Ken Osato, etc.)

Inflation?

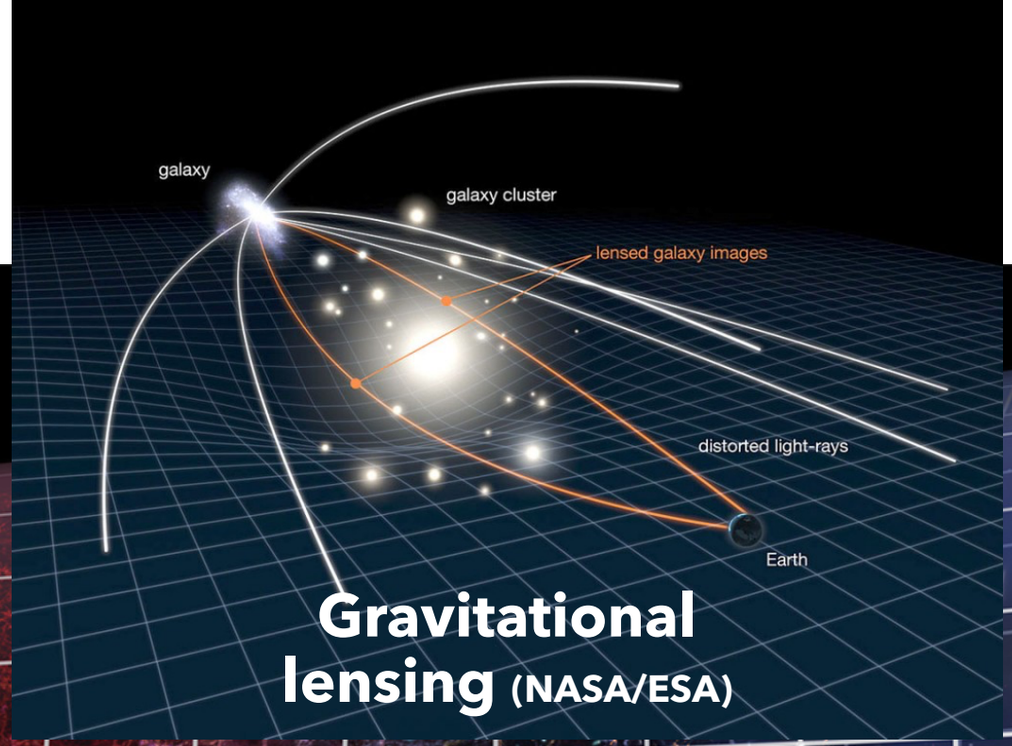

Gravitational lensing (NASA/ESA)

Galaxy Cluster

(MACS0416.1-2403)

$$\Omega_m = \Omega_{\rm DM} + \Omega_b, \Omega_\Lambda, w, h, S_8, \Sigma m_\nu$$

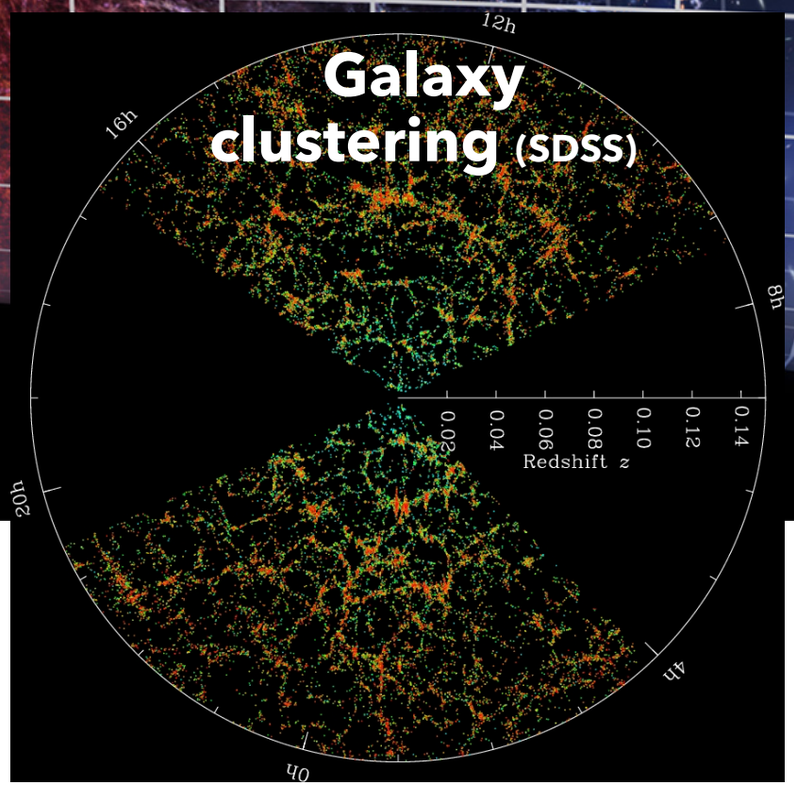

Galaxy clustering (SDSS)

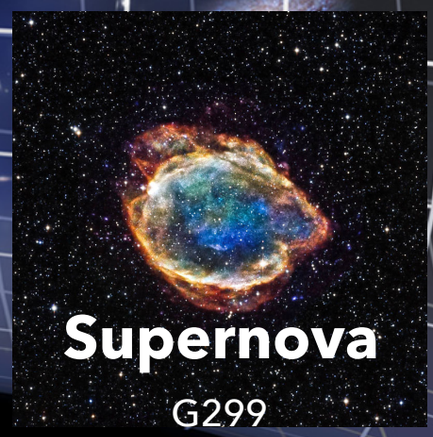

Supernova

G299

ESO/ELT

Landscapes in 2020s cosmology

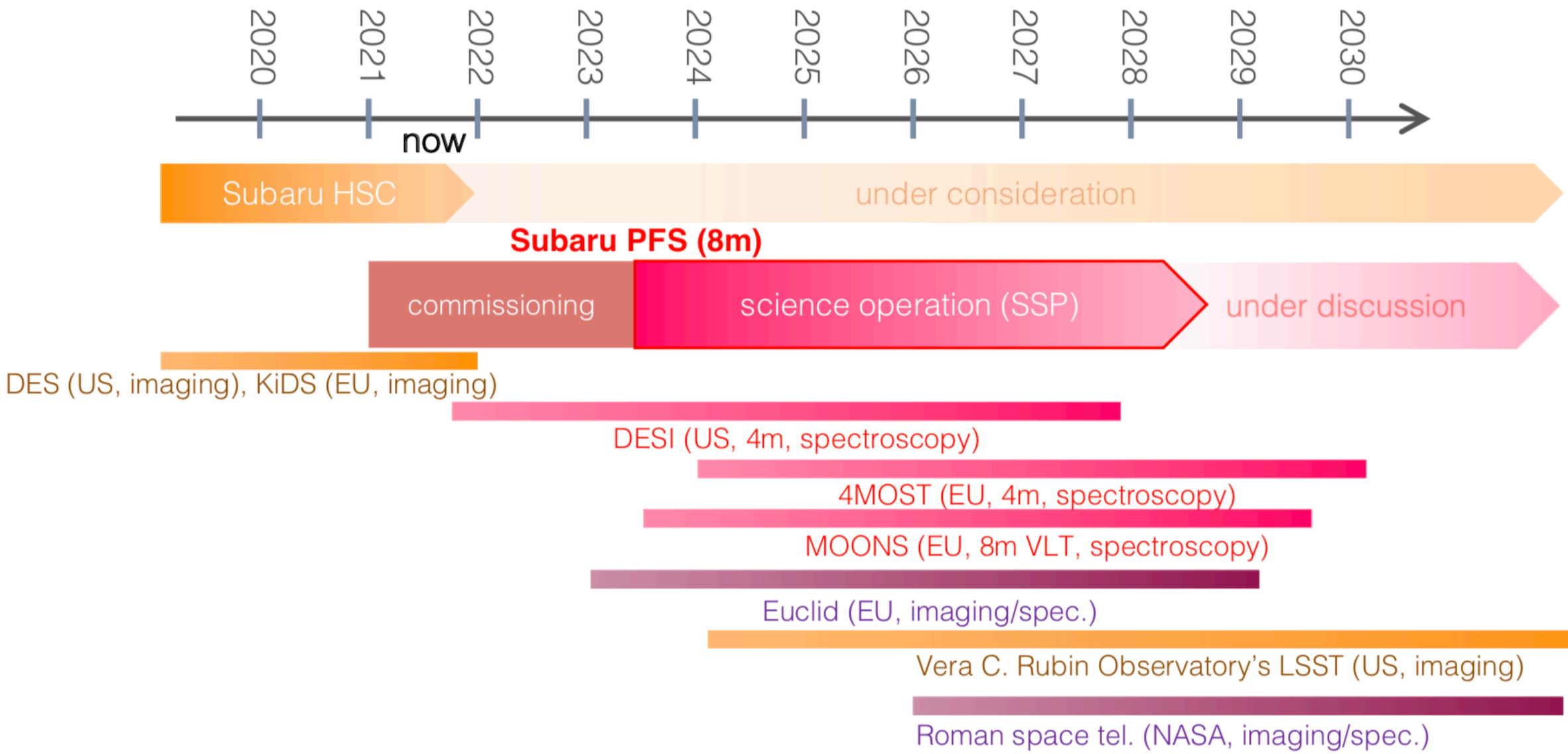

Takada san's talk

GALAXY INTRINSIC ALIGNMENT

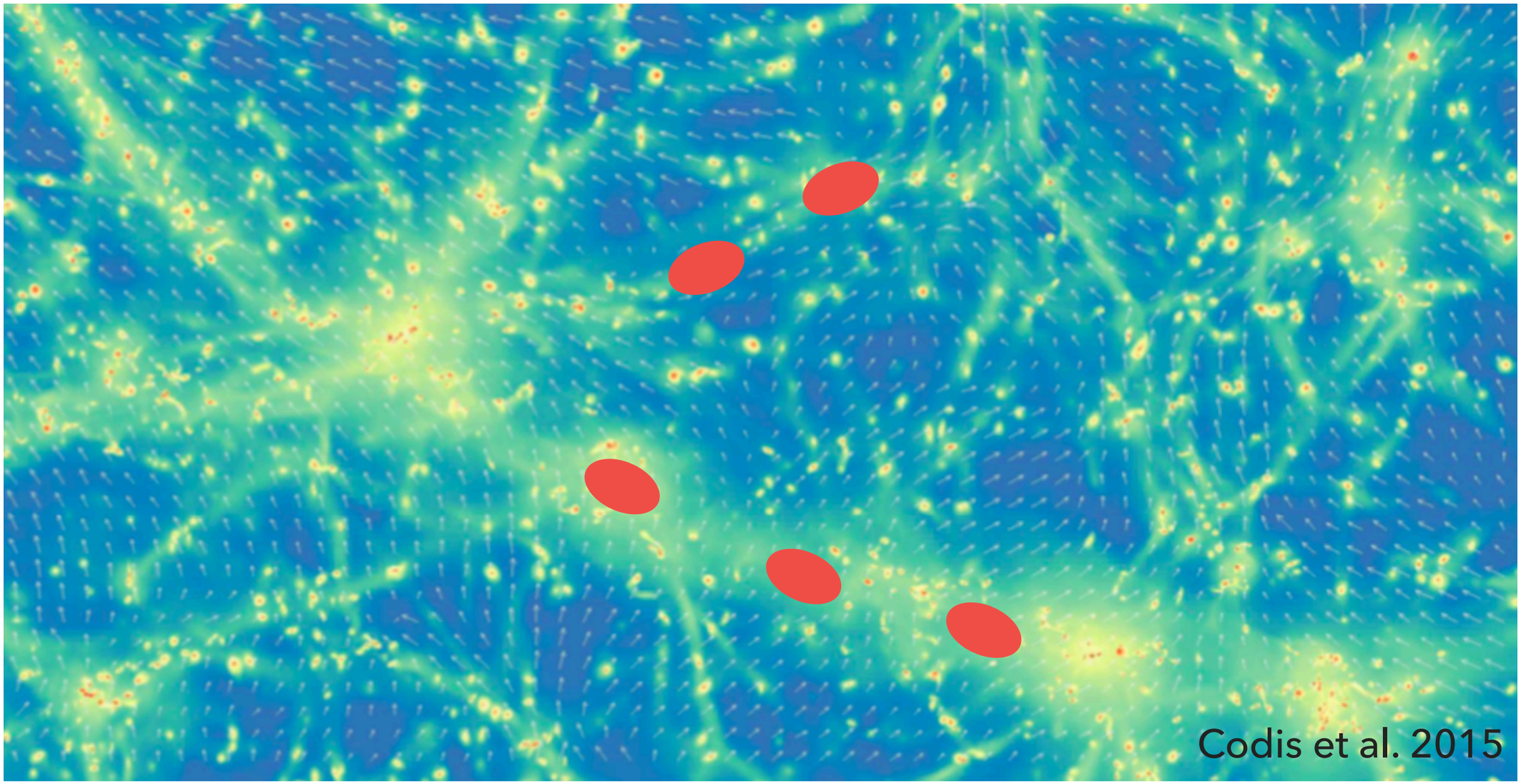

- **Challenge** – contaminates weak lensing cosmology
- **Opportunity** – probe of cosmology and galaxy formation physics

GALAXY INTRINSIC ALIGNMENT – THEORIES

$$\gamma^I = -\frac{C_1}{4\pi G}(\nabla_x^2 - \nabla_y^2, 2\nabla_x\nabla_y)\mathcal{S}[\Psi_P]$$

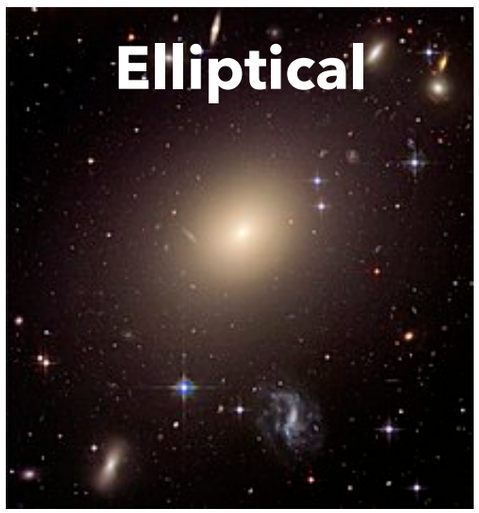

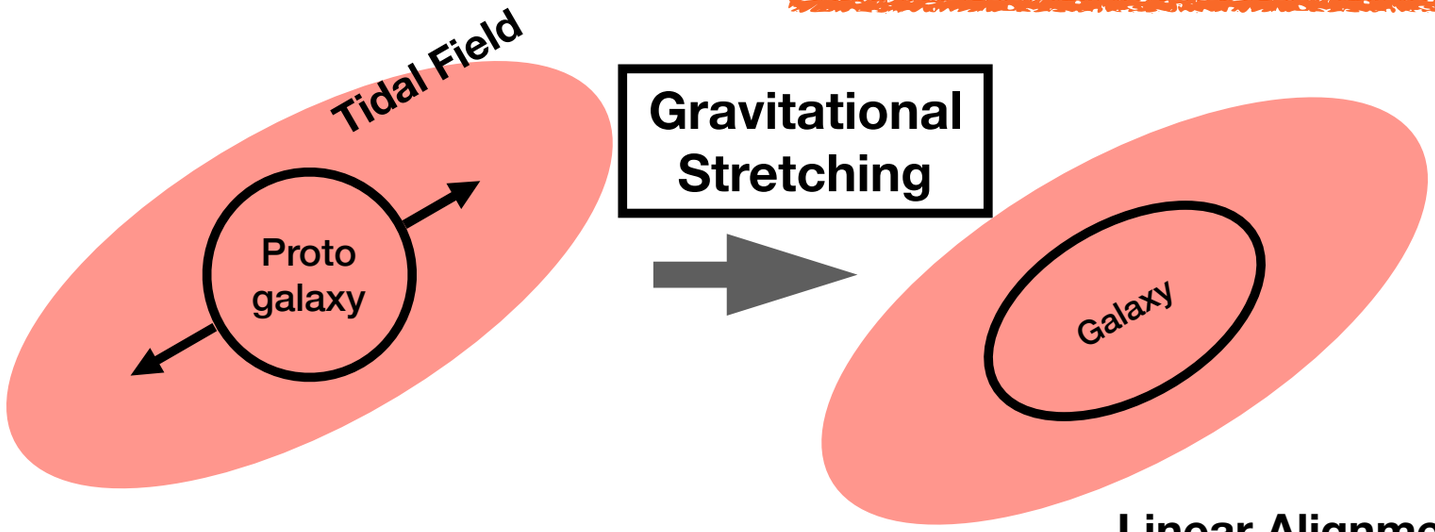

Linear Alignment

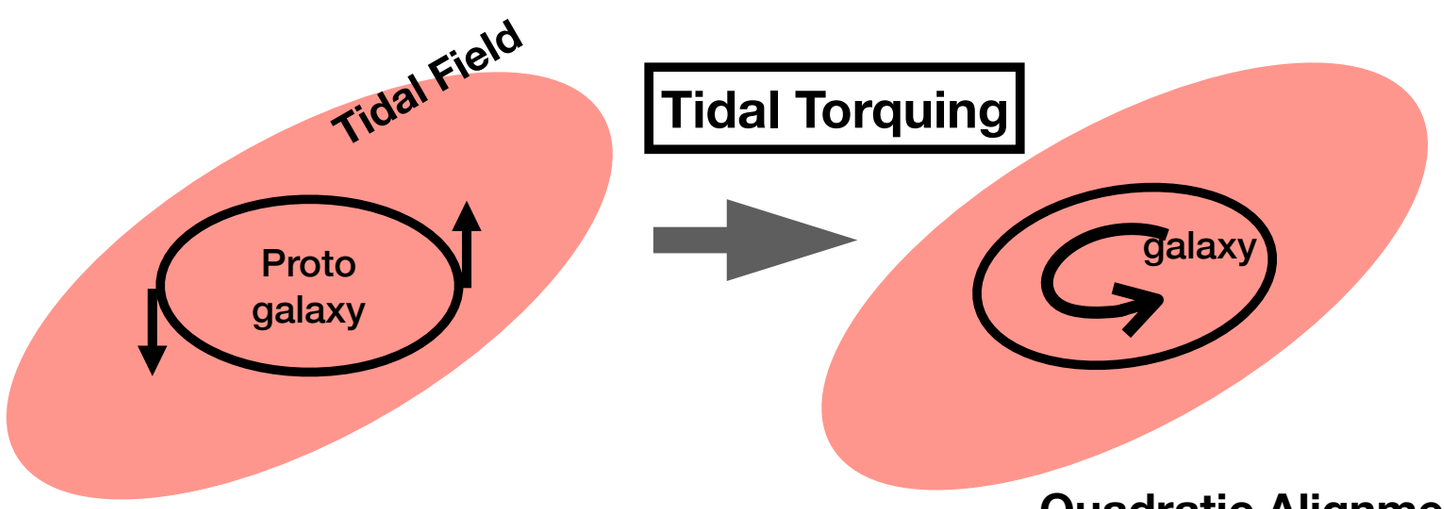

Quadratic Alignment

$$\gamma^I_{(+,\times)} = C_2(T^2_{1i} - T^2_{2i}, 2T_{1i}T_{2i})$$

Catelan+2001, Hirata & Seljak 2004, White 1984

Source

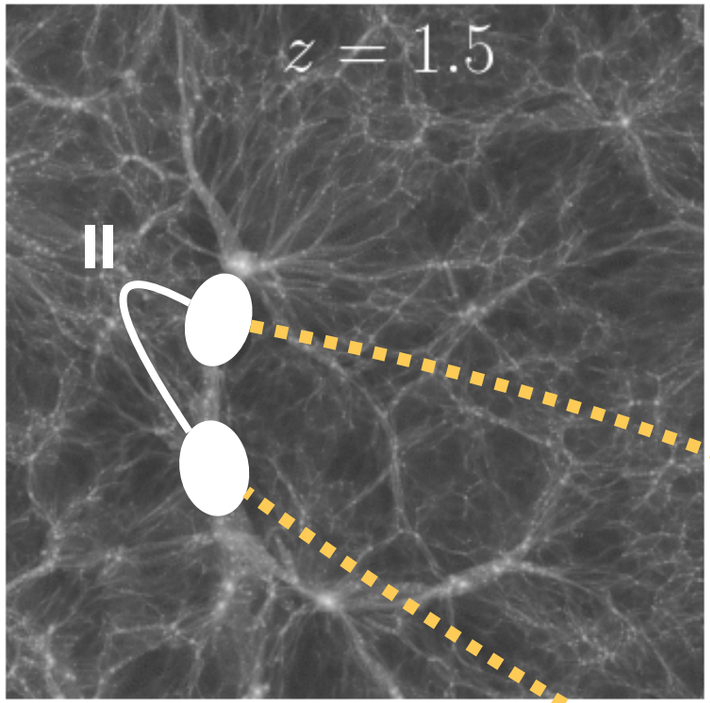

Structure Growth and Accelerating Expansion

Lens: matter along line of sight

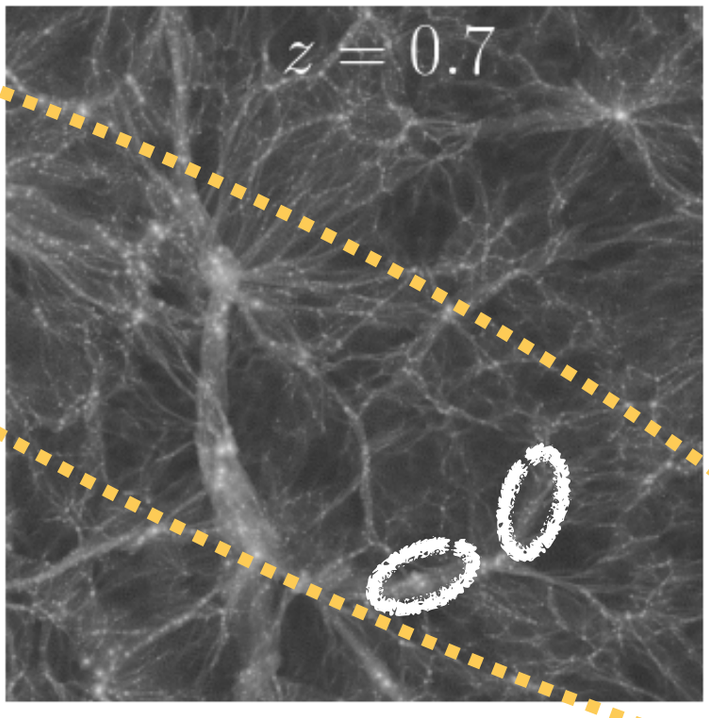

Observed Images

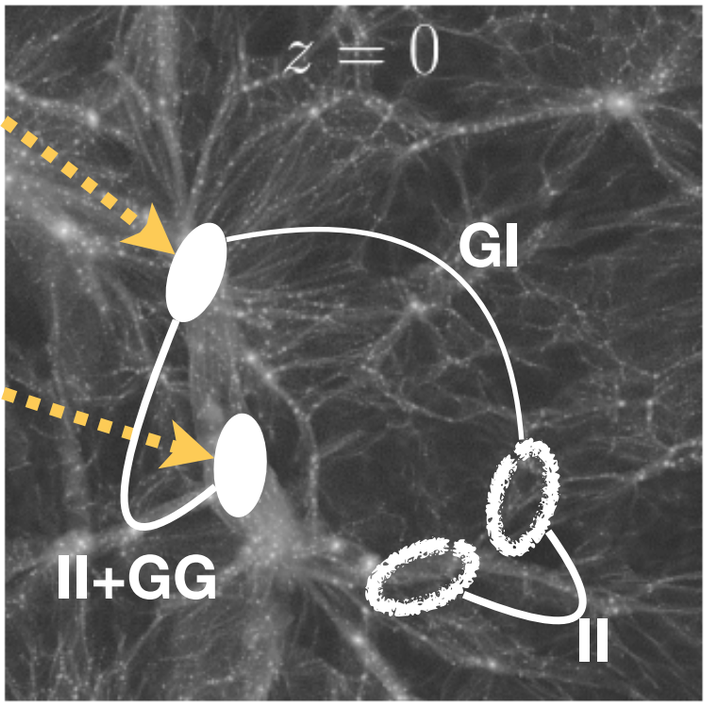

II: intrinsic alignment
GI: intrinsic alignment
GG: cosmic shear

Galaxy intrinsic alignment – Primary contamination of cosmic shear cosmology

(Hirata & Seljak 2004, Troxel+2015)

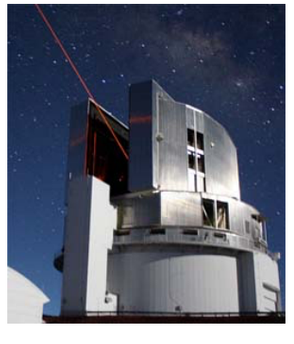

Krause+2015

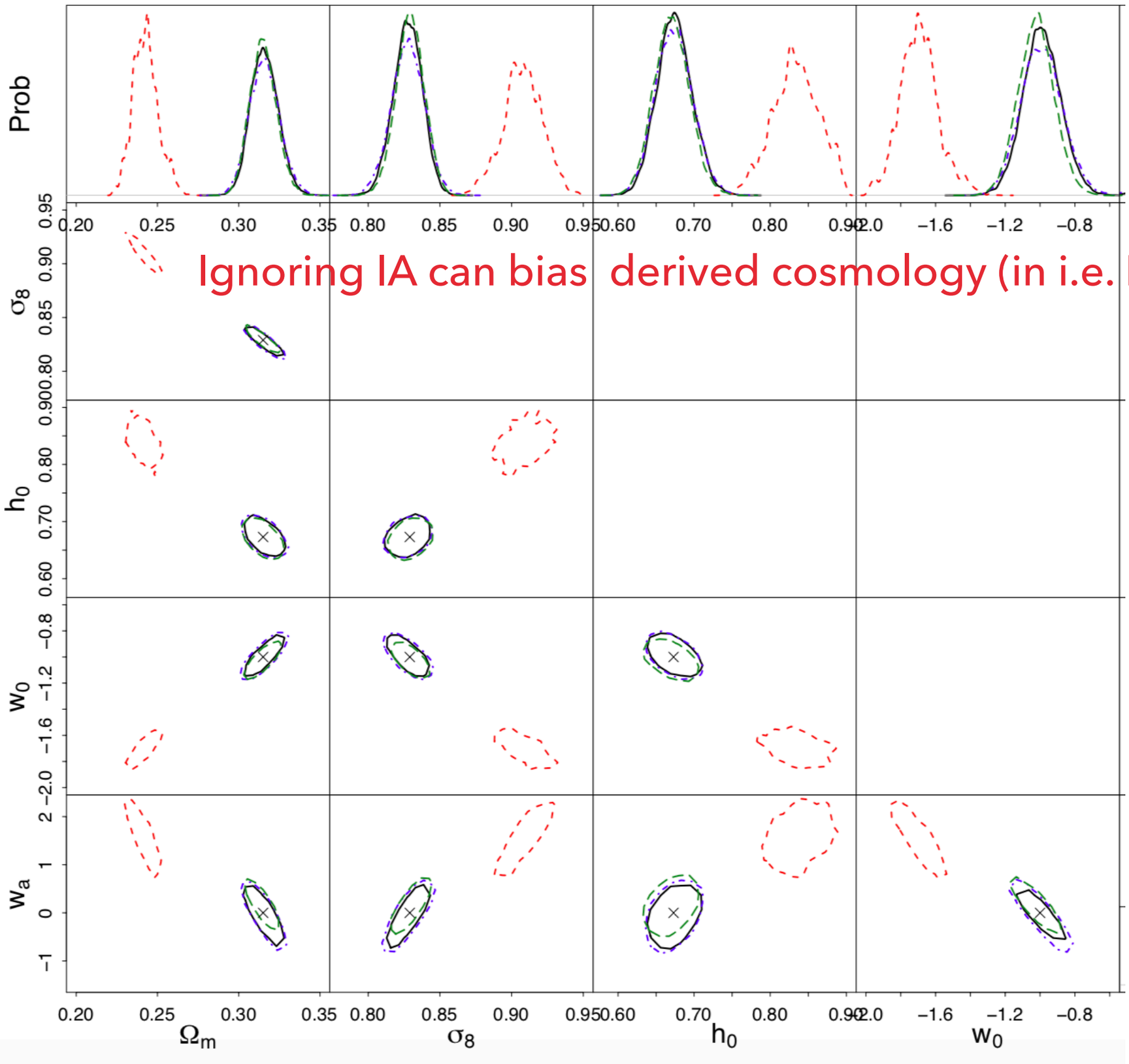

Ignoring IA can bias derived cosmology (in i.e. Euclid WL)

INTRINSIC ALIGNMENT – OBSERVATIONS

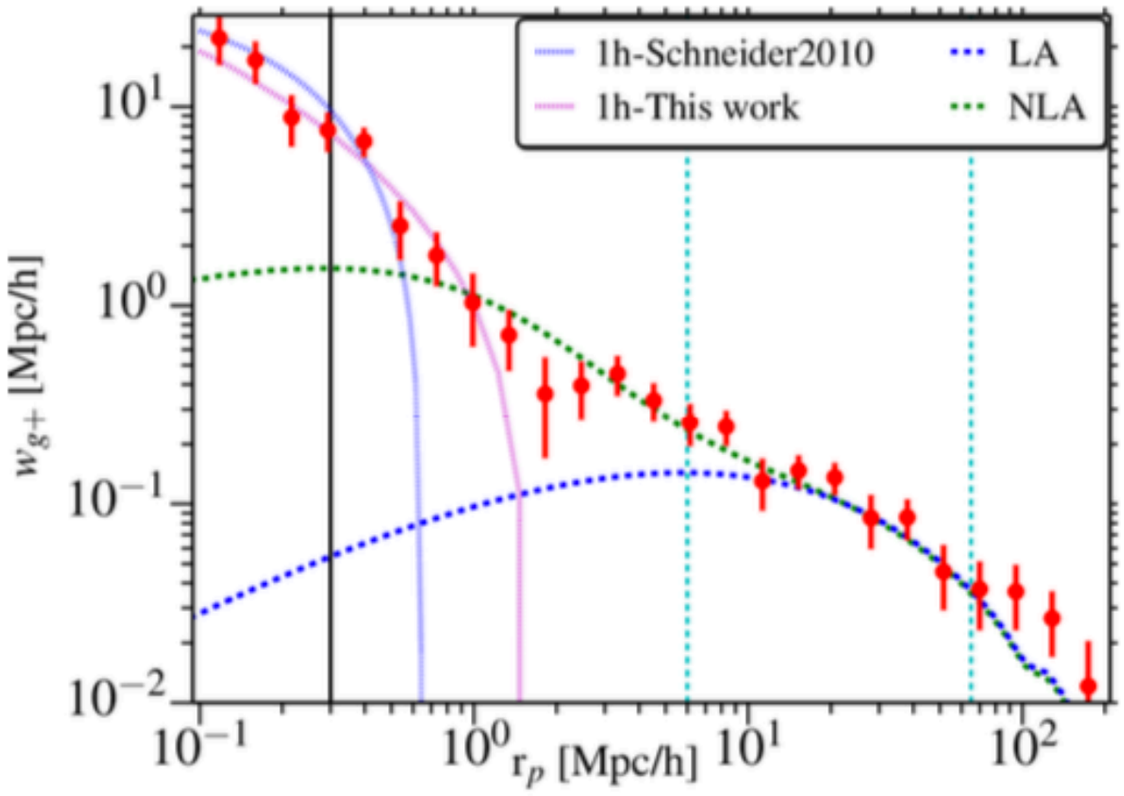

Luminous red galaxies – clear IA signal shown by the correlation function between galaxy positions and intrinsic ellipticities

Singh et al. 2015

Mandelbaum+2011, Yao+2020

Blue star-forming galaxies – no clear IA signal detected so far

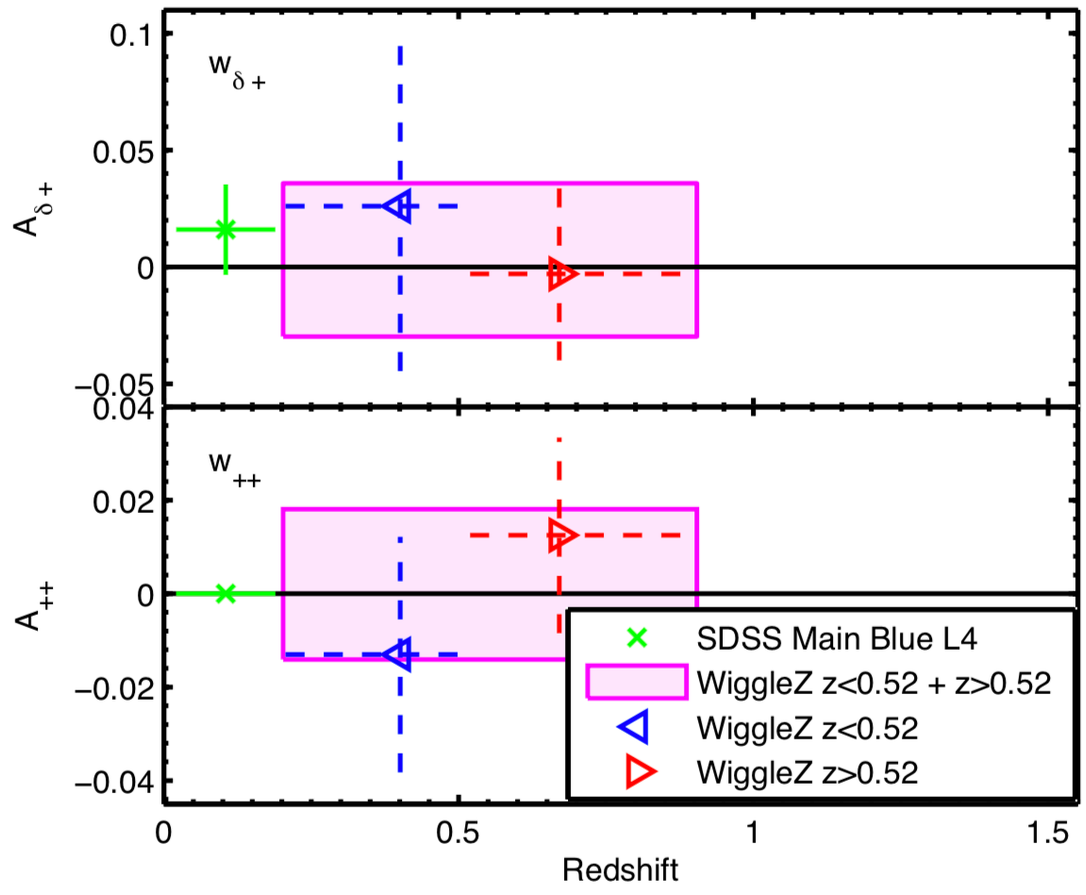

INTRINSIC ALIGNMENT – OBSERVATIONS

Non-linear and baryonic physics dominates !

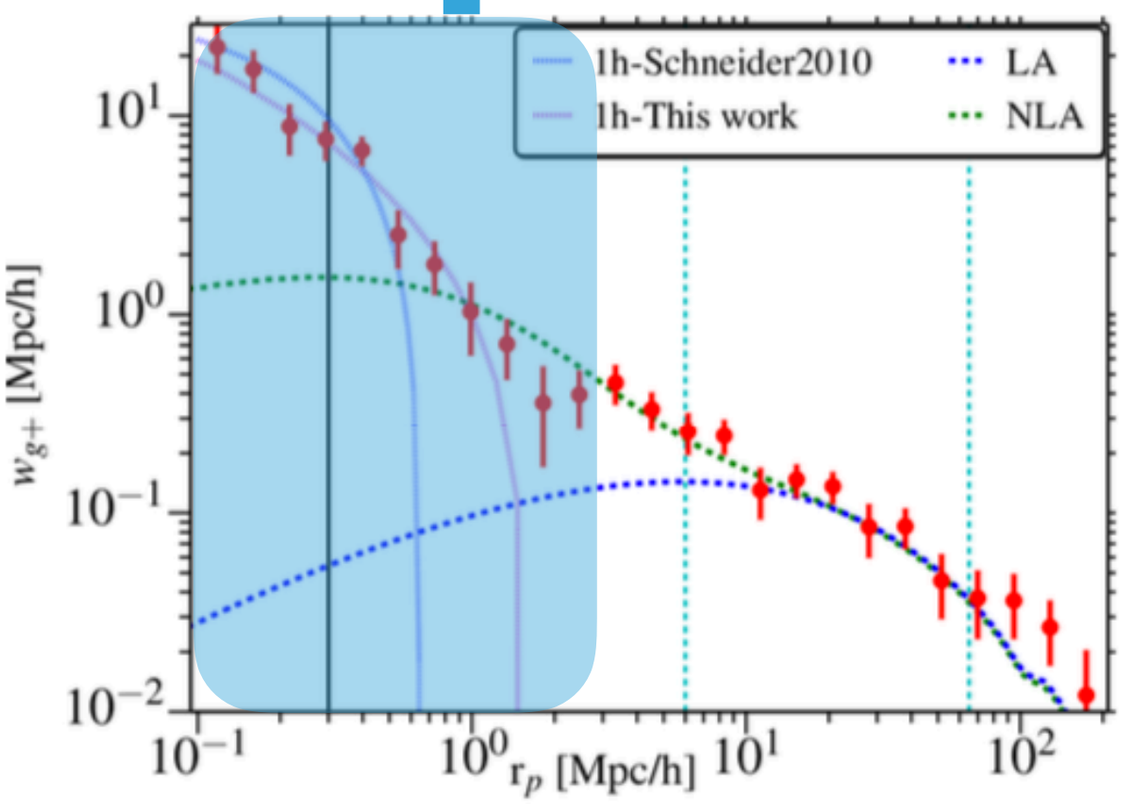

Luminous red galaxies – clear IA signal shown by the correlation function between galaxy positions and intrinsic ellipticities

Singh et al. 2015

Mandelbaum+2011, Yao+2020

Blue star-forming galaxies – no clear IA signal detected so far

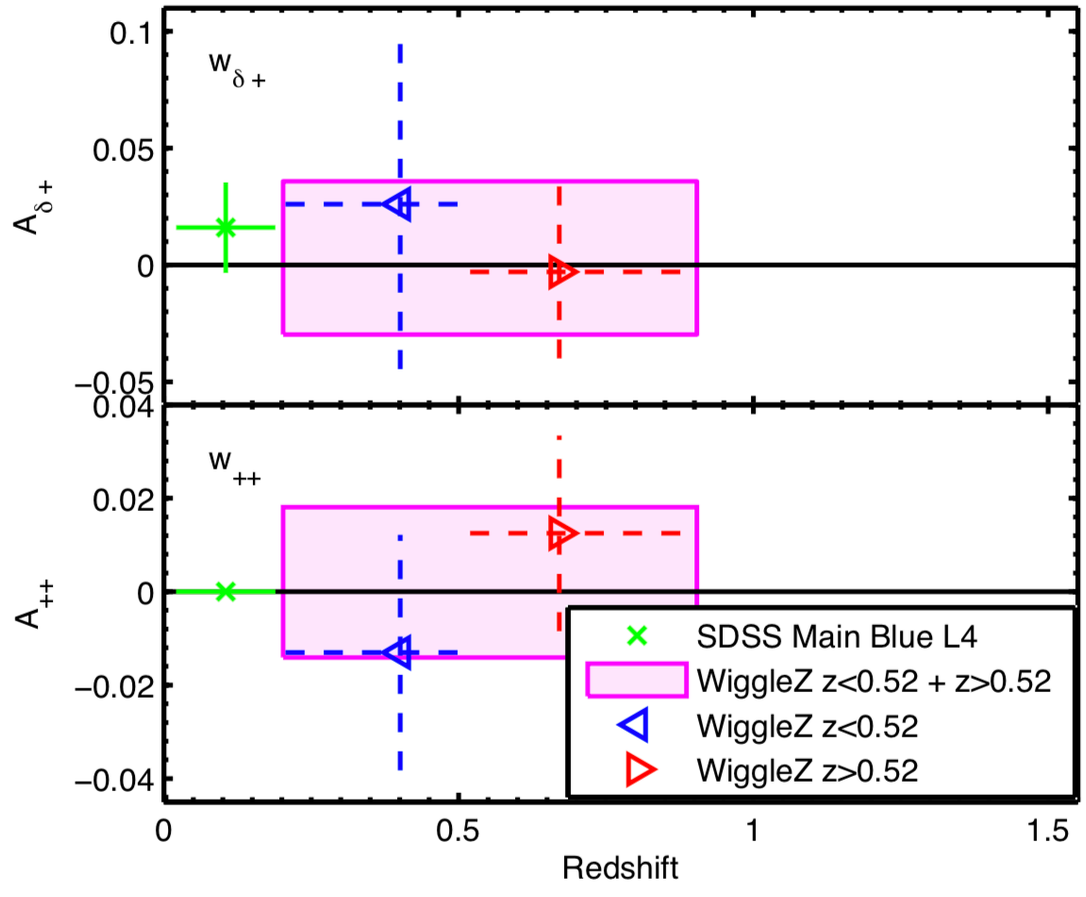

SIMULATIONS

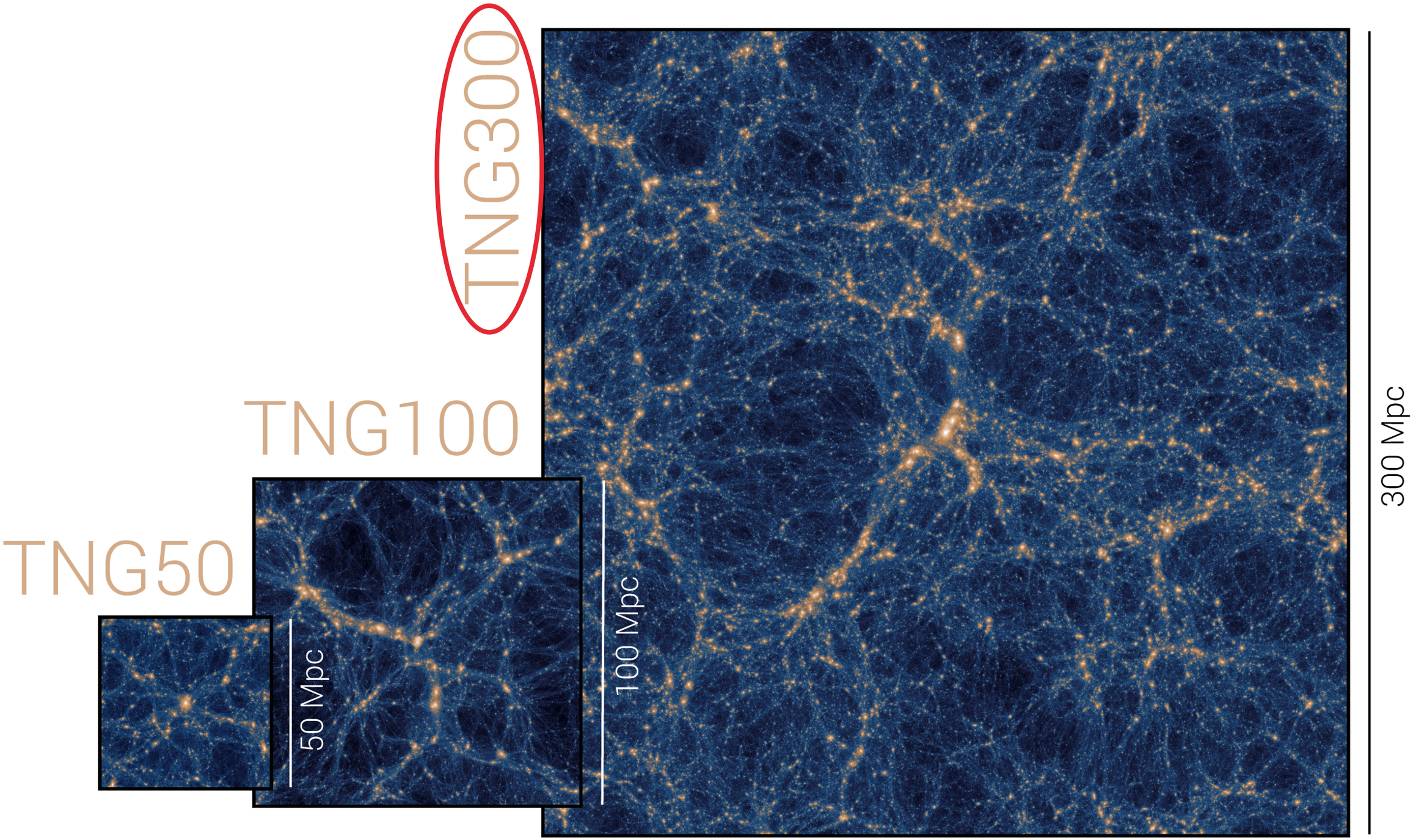

IA POWER SPECTRUM

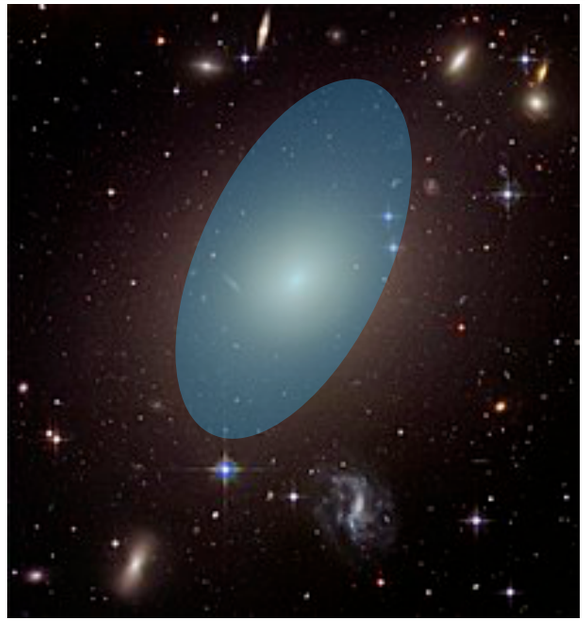

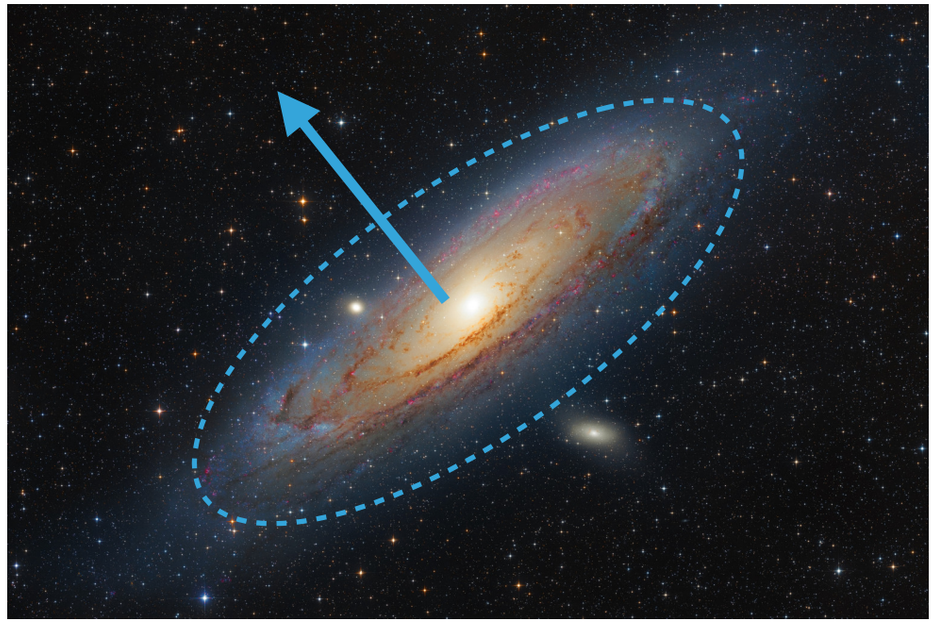

$$\epsilon_+ \equiv \frac{I_{11} - I_{22}}{I_{11} + I_{22}}, \epsilon_\times \equiv \frac{2I_{12}}{I_{11} + I_{22}}$$

$$\epsilon_+ \equiv -\frac{\hat{L}_1^2 - \hat{L}_2^2}{1 + \hat{L}_3^2}, \epsilon_\times \equiv -\frac{2\hat{L}_1^2\hat{L}_2^2}{1 + \hat{L}_3^2}$$

$$\gamma_{+,\times} = \epsilon_{+,\times}/(2\mathcal{R}), \text{ where } \mathcal{R} \equiv 1 - \langle \epsilon_i^2 \rangle$$

$$\gamma_E(\boldsymbol{k}) = \gamma_+(\boldsymbol{k}) \cos 2\phi_{\boldsymbol{k}} + \gamma_\times(\boldsymbol{k}) \sin 2\phi_{\boldsymbol{k}},$$
$$\gamma_B(\boldsymbol{k}) = -\gamma_+(\boldsymbol{k}) \sin 2\phi_{\boldsymbol{k}} + \gamma_\times(\boldsymbol{k}) \cos 2\phi_{\boldsymbol{k}},$$

Kurita+2021, Shi et al. 2021a

$$\langle \gamma_E(\boldsymbol{k}) \gamma_E(\boldsymbol{k}') \rangle \equiv (2\pi)^3 \delta_D(\boldsymbol{k} + \boldsymbol{k}') P_{EE}(\boldsymbol{k}),$$
$$\langle \gamma_E(\boldsymbol{k}) \delta_m(\boldsymbol{k}') \rangle \equiv (2\pi)^3 \delta_D(\boldsymbol{k} + \boldsymbol{k}') P_{\delta E}(\boldsymbol{k}),$$
$$\langle \gamma_E(\boldsymbol{k}) \delta_g(\boldsymbol{k}') \rangle \equiv (2\pi)^3 \delta_D(\boldsymbol{k} + \boldsymbol{k}') P_{gE}(\boldsymbol{k}),$$

Merits of IA Power Spectrum

- Scale dependence of IA
- Full information on 2pt statistics
- High S/N ratio

INTRINSIC ALIGNMENT – M_* AND REDSHIFT DEPENDENCE

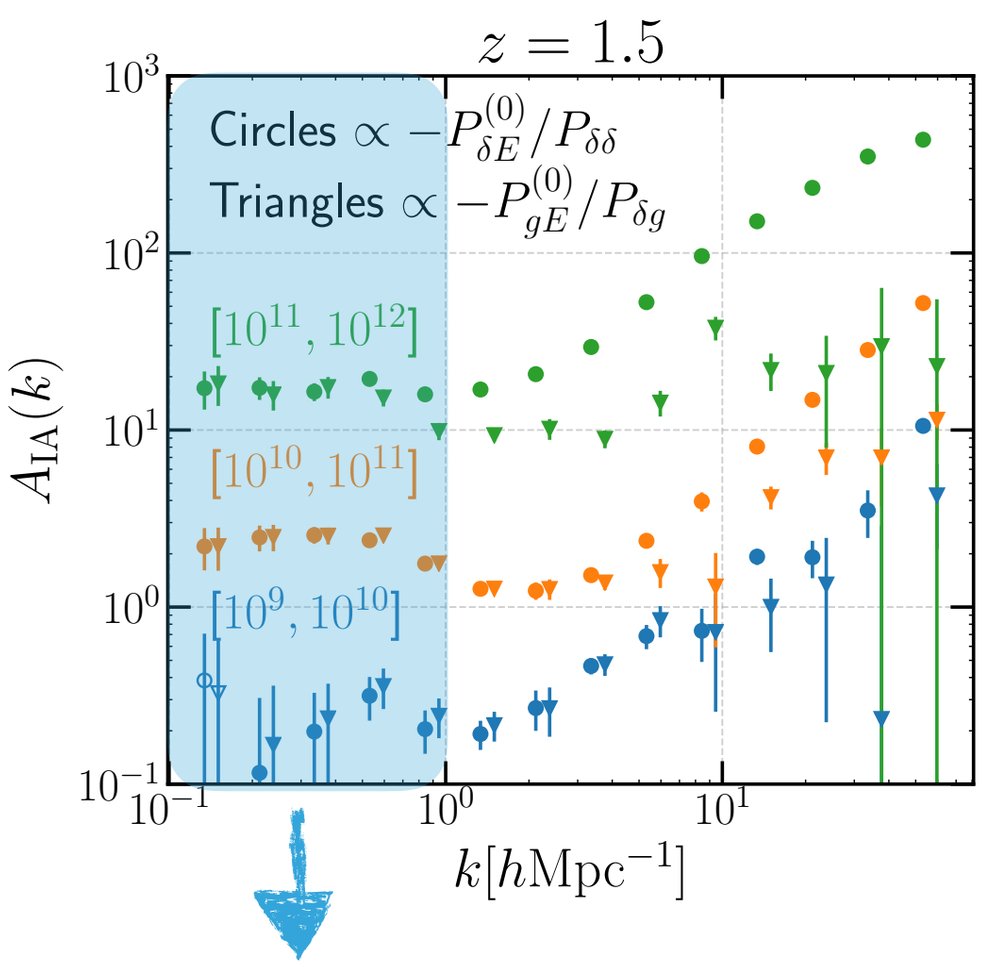

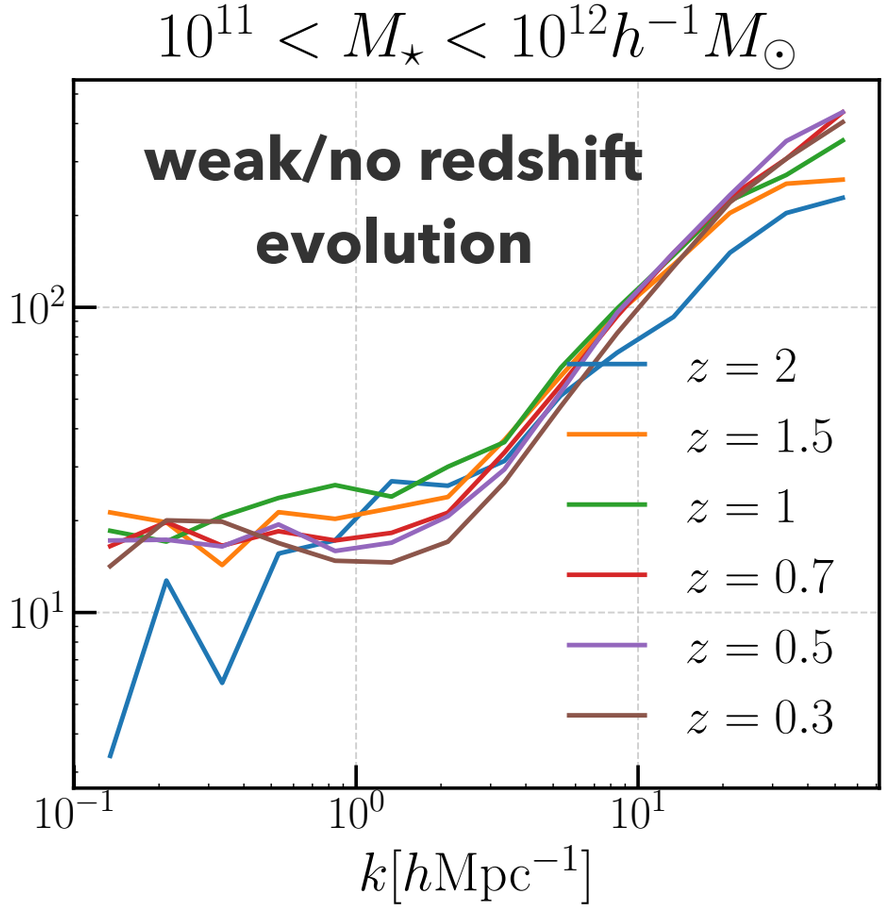

Consistent with NLA prediction

$$P_{\delta E}(k,\mu) = -A_{\rm IA} C_1 \rho_{\rm cr0} \frac{\Omega_{\rm m}}{D(z)} (1-\mu^2) P_{\delta\delta}(k,z)$$

INTRINSIC ALIGNMENT – ENVIRONMENT DEPENDENCE

Matter field
X
galaxy (shape/spin) shear

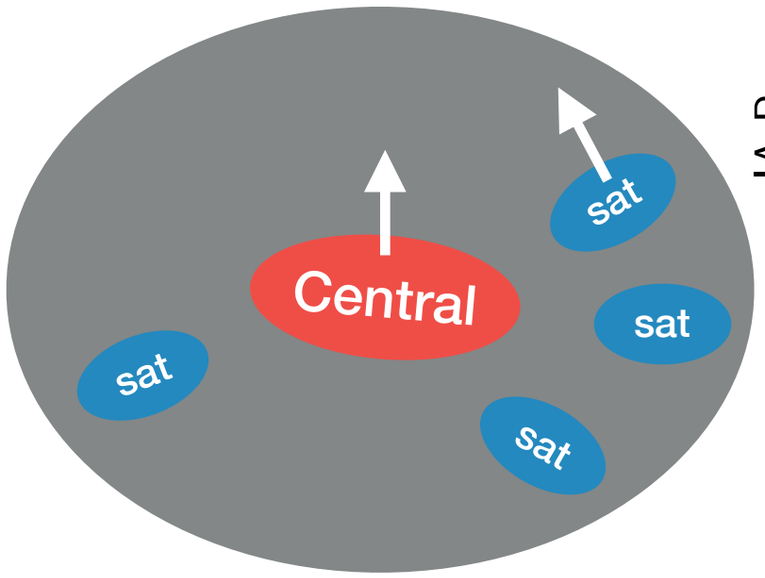

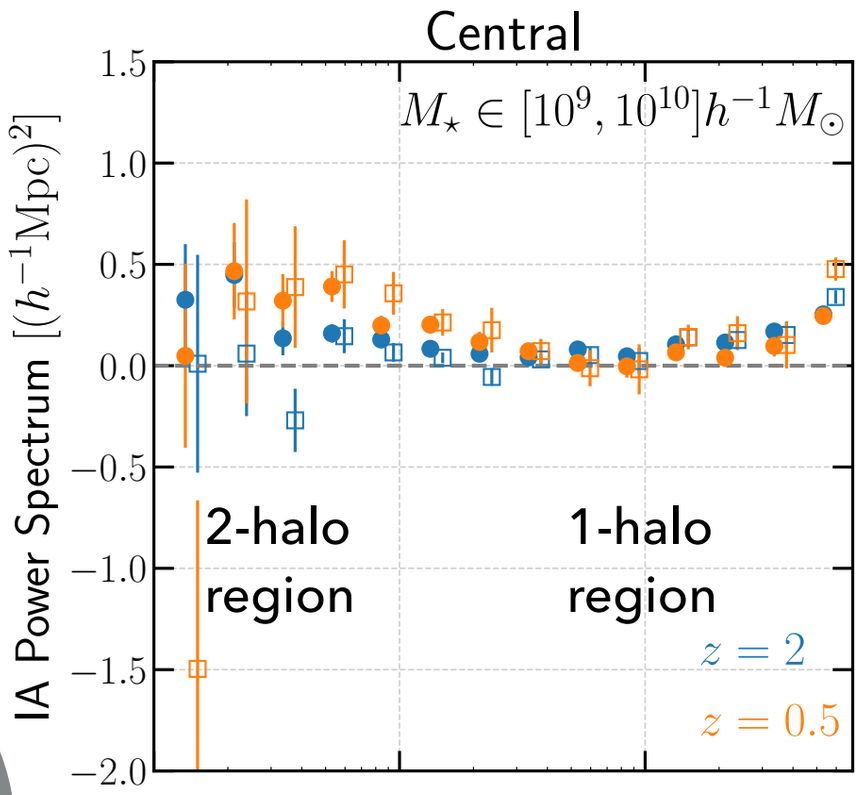

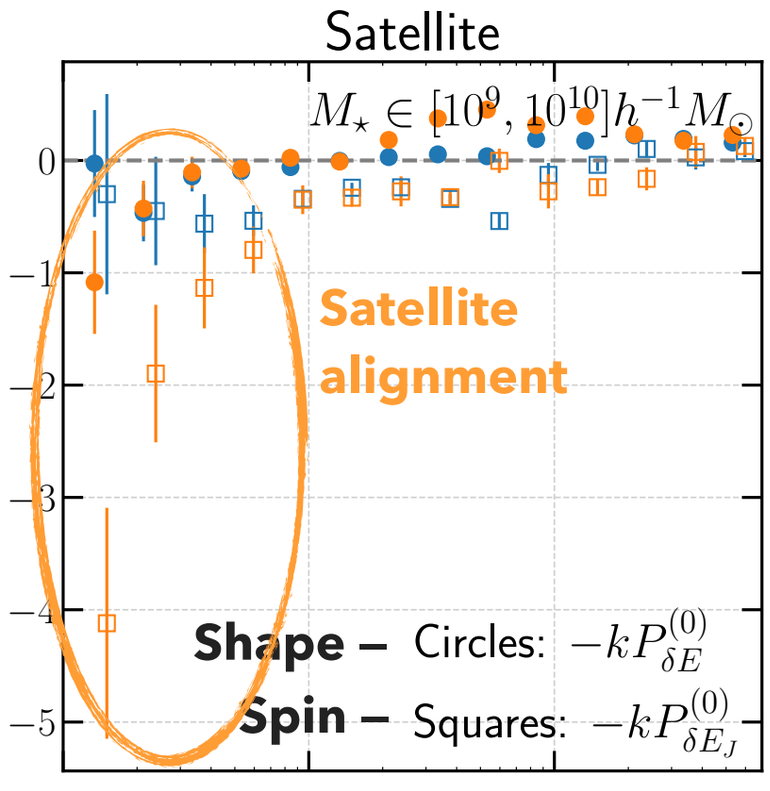

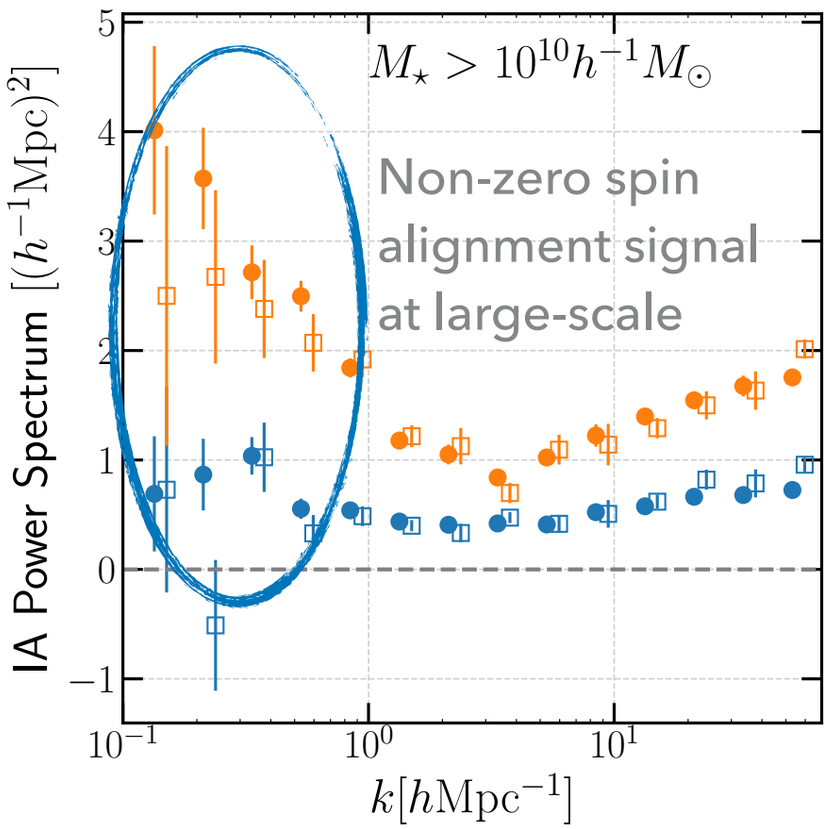

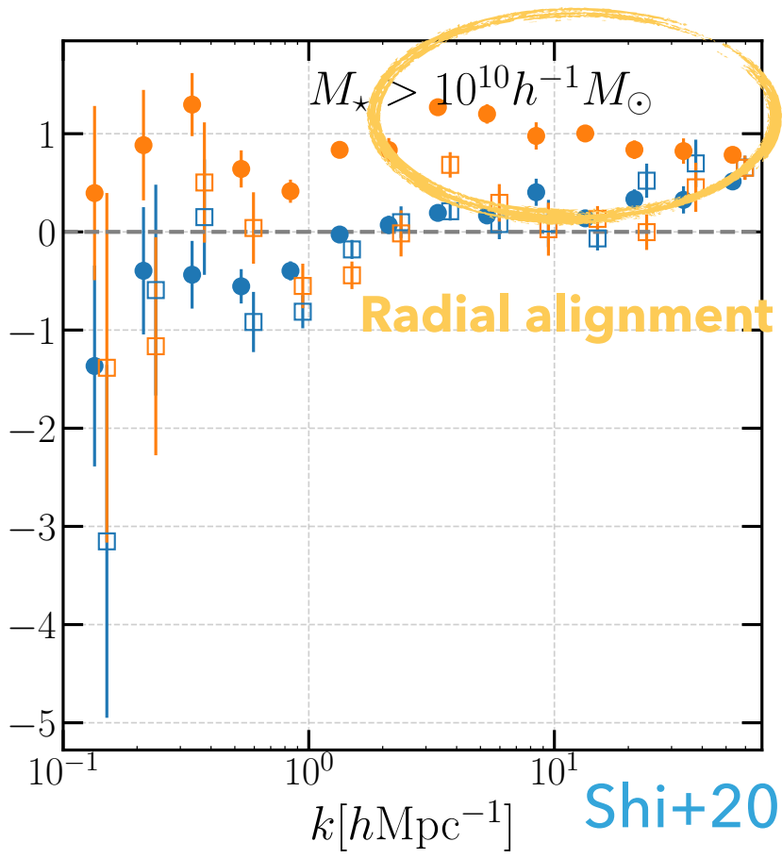

Shi+2021a

INTRINSIC ALIGNMENT – MORPHOLOGICAL DEPENDENCE

Matter field
X
galaxy (shape/spin) shear

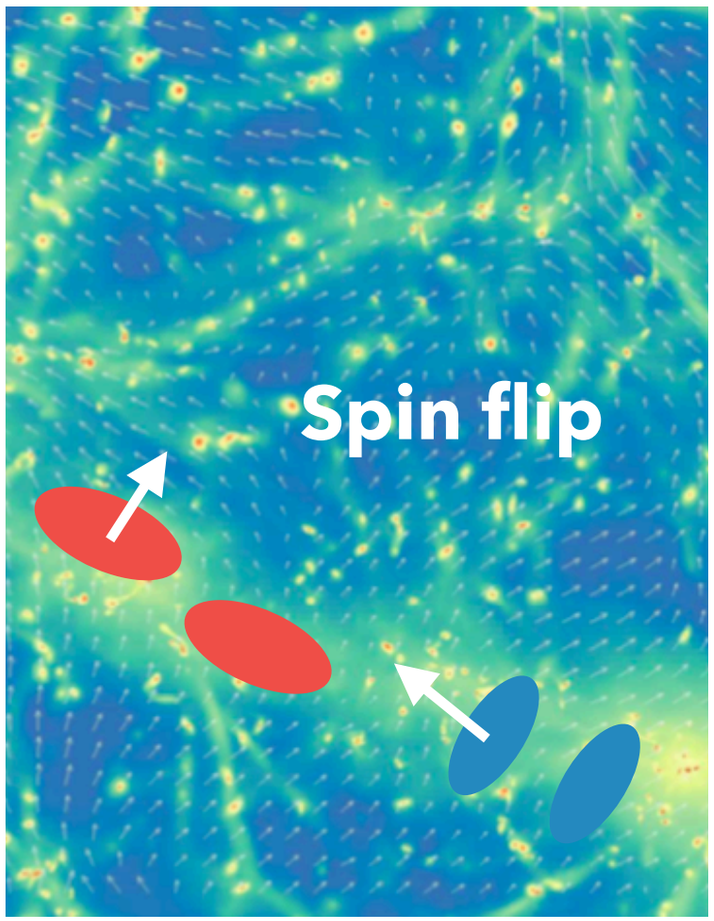

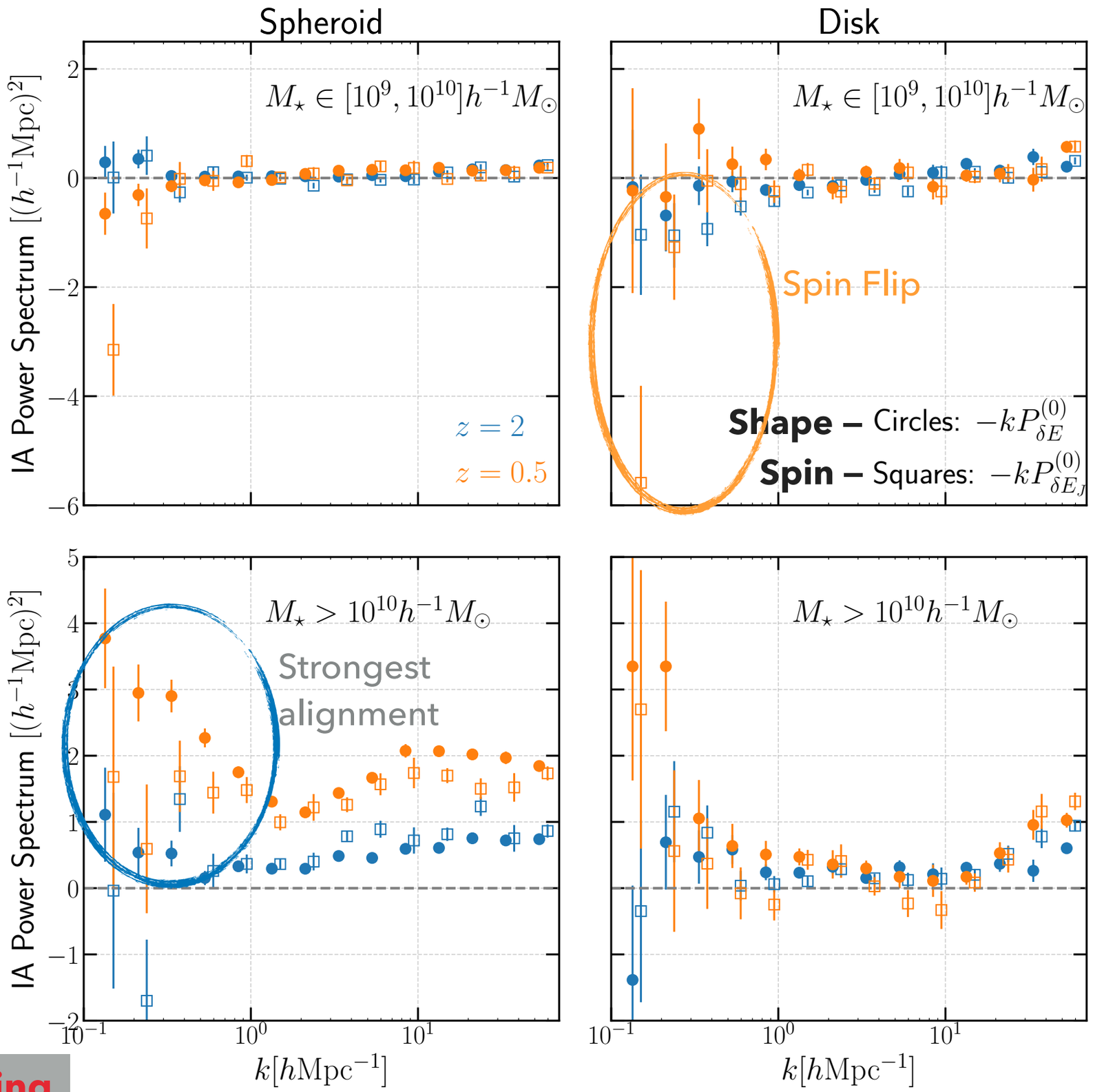

IA is useful for distinguishing the galaxy formation models!

Shi+2021a

INTRINSIC ALIGNMENT – SYNERGY BETWEEN IMAGE AND SPEC SURVEYS

~LRGs

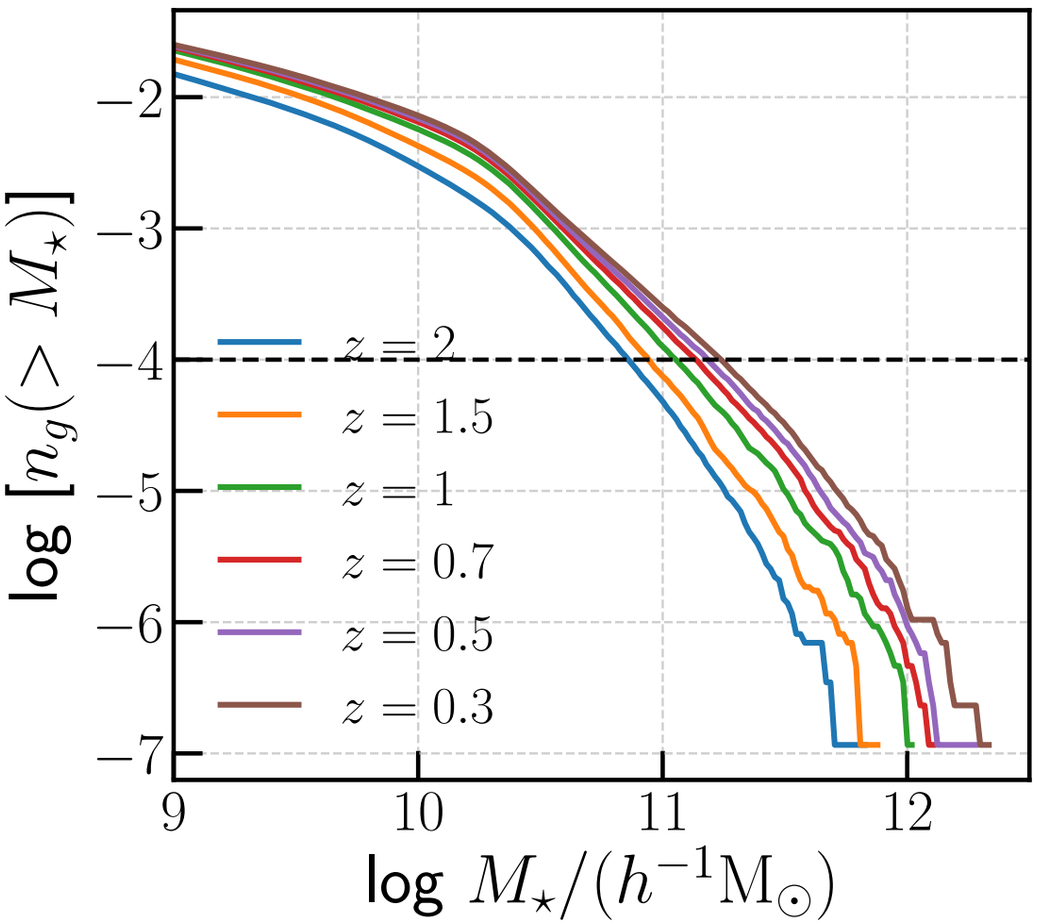

~ELGs

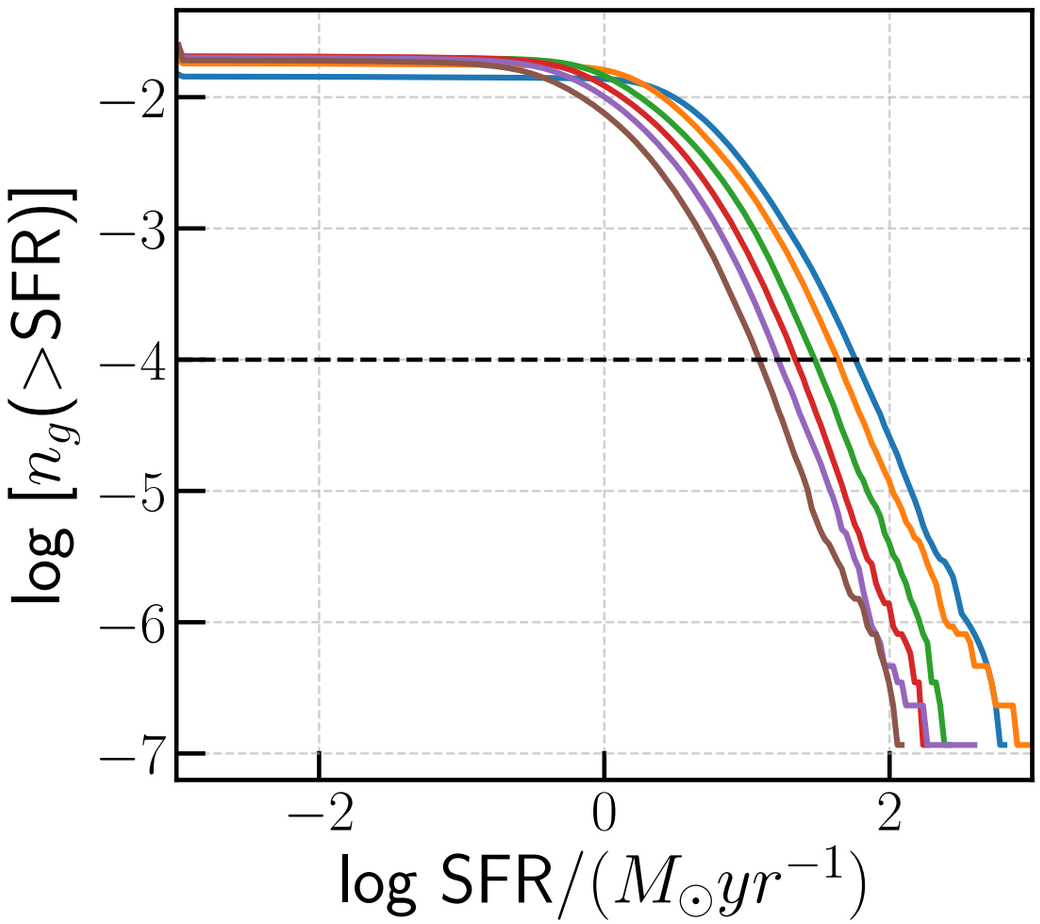

Shi+2021a

INTRINSIC ALIGNMENT – SYNERGY BETWEEN IMAGE AND SPEC SURVEYS

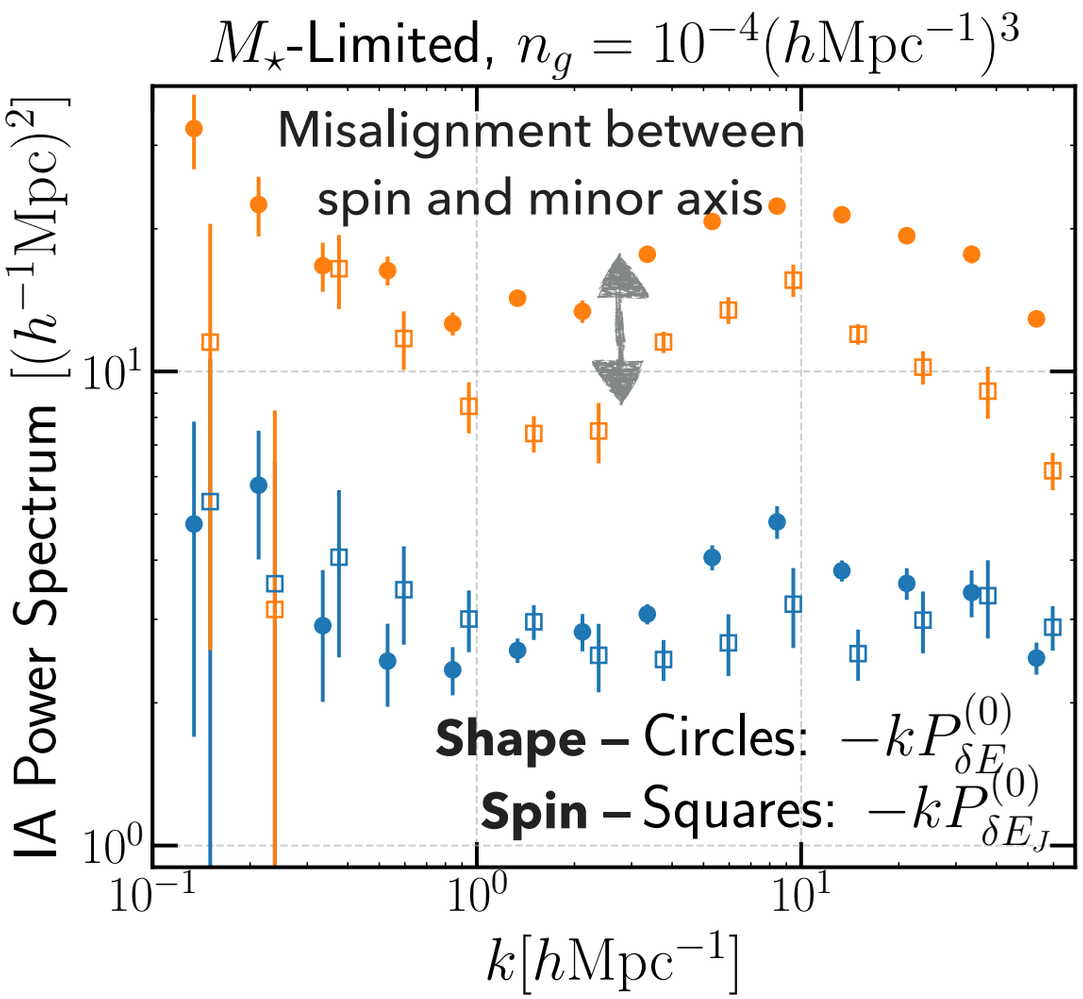

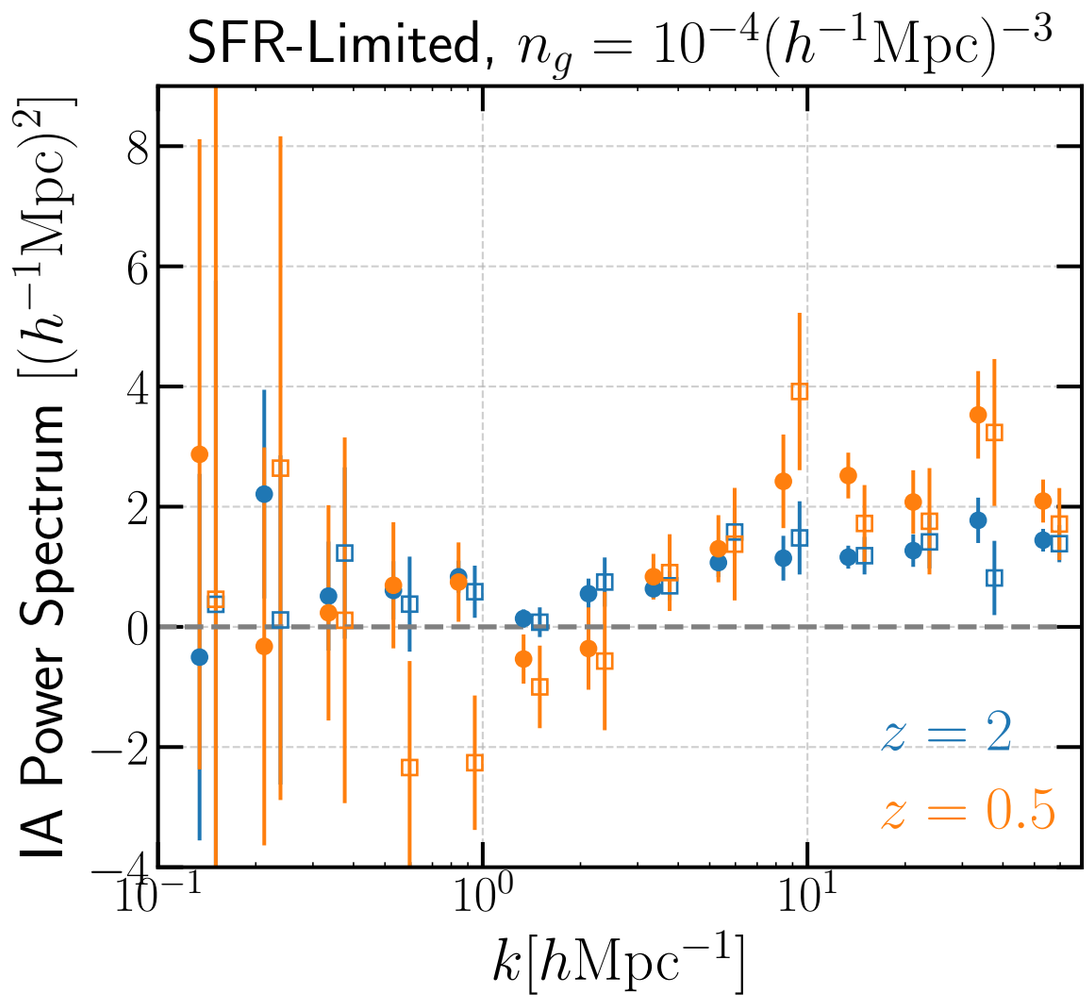

Shi+2021a

INTRINSIC ALIGNMENT – SYNERGY BETWEEN IMAGE AND SPEC SURVEYS

ELGs traced density field cross correlate with LRGs ellipticity field

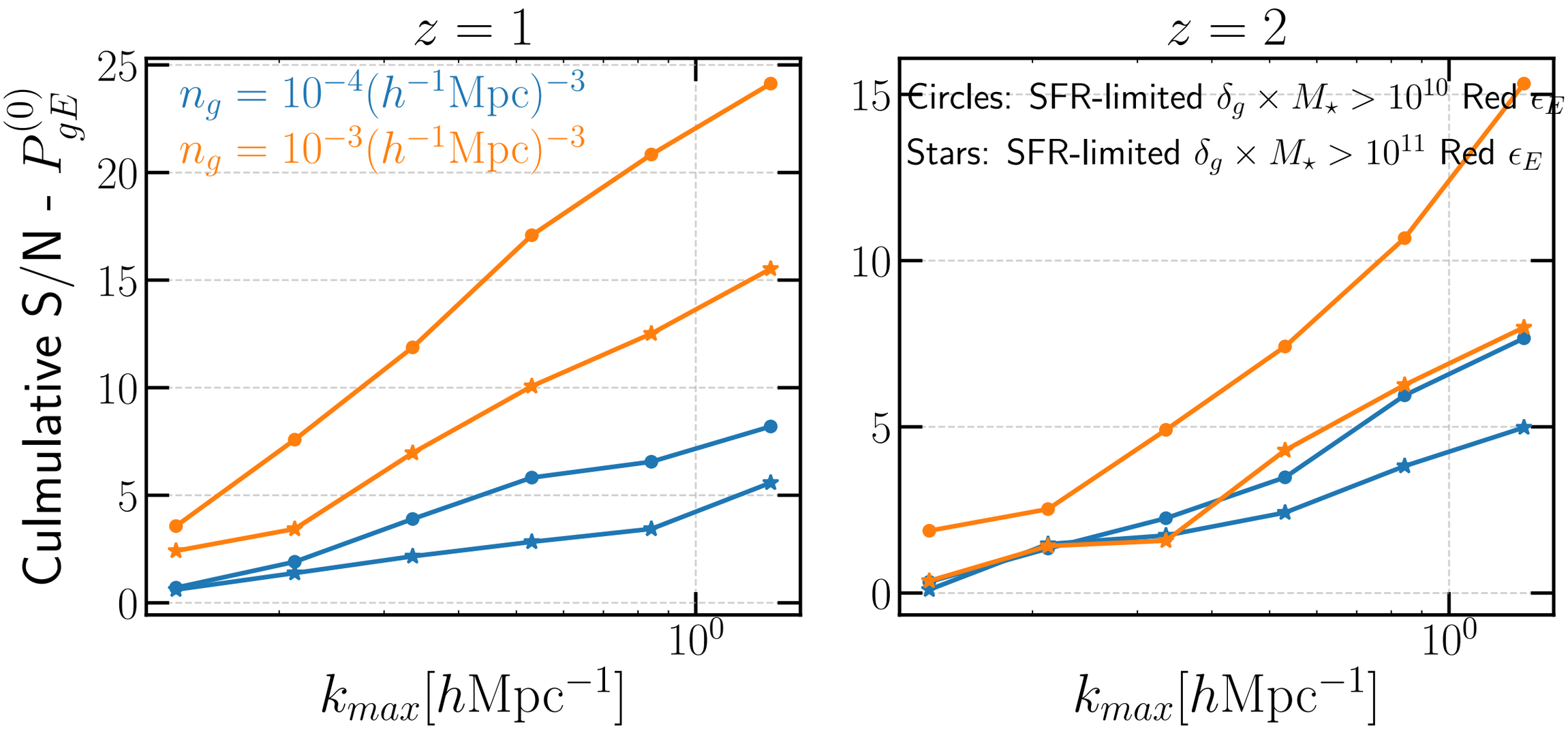

See Benjamin's talk for prediction on high-z IA in PFS galaxy survey

$$\left(\frac{S}{N}\right)^2 \equiv \sum_{k_i=k_{\rm min}}^{k_{\rm max}} \bar{P}_{gE}^{(0)}(k_i)\,[\mathbf{C}]_{ij}^{-1}\,\bar{P}_{gE}^{(0)}(k_j)$$

Shi+2021a

GALAXY INTRINSIC ALIGNMENT

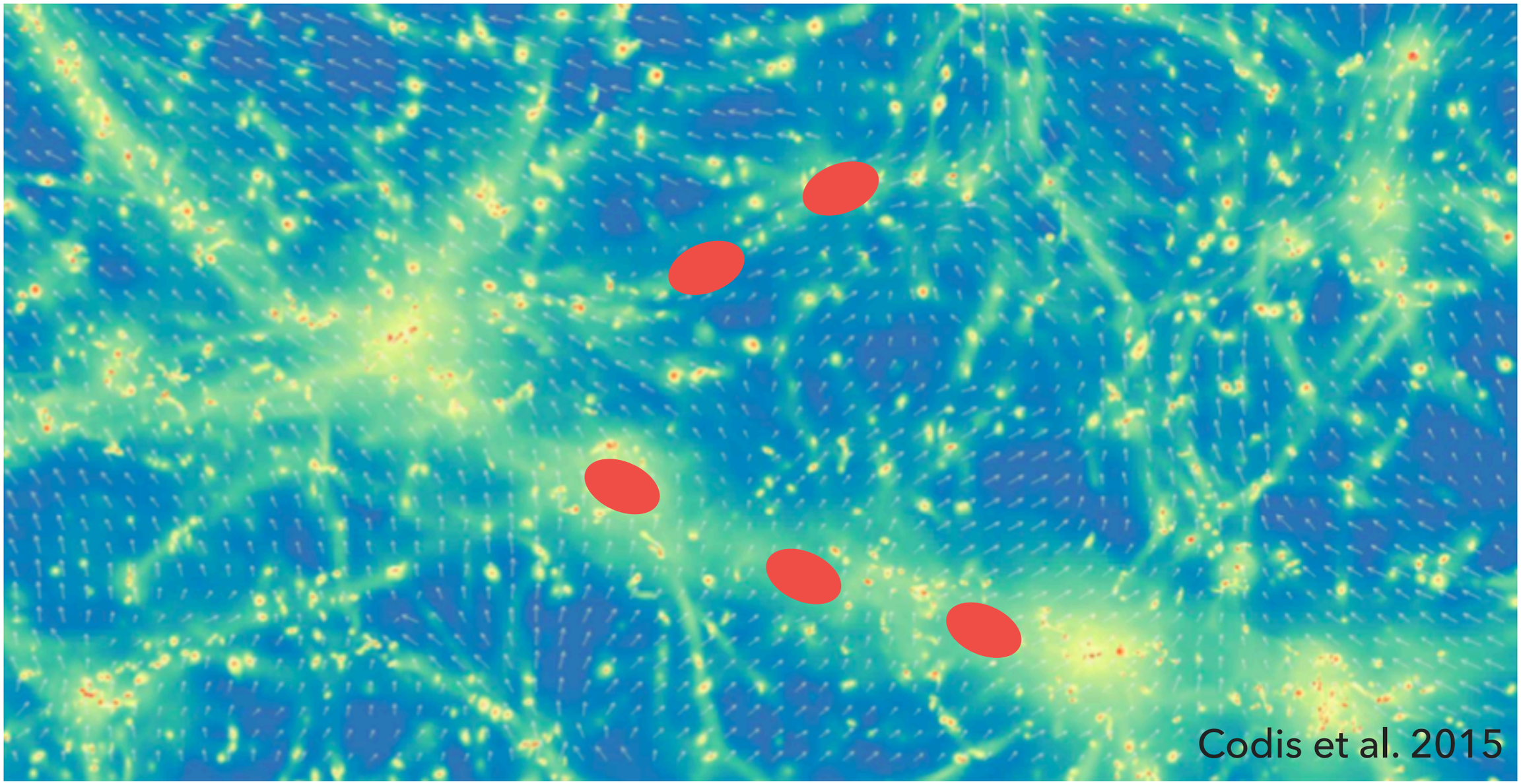

- **Challenge** – contaminates weak lensing cosmology
- **Opportunity** – probe of cosmology and galaxy formation physics

INTRINSIC ALIGNMENT – PROBE OF COSMOLOGY

- Complementary probe of Baryonic Acoustic Oscillation, Redshift Space Distortion (Chisari+2013, Taruya & Okumura2020)
- ~1.5 tighter constraint by combing with IA

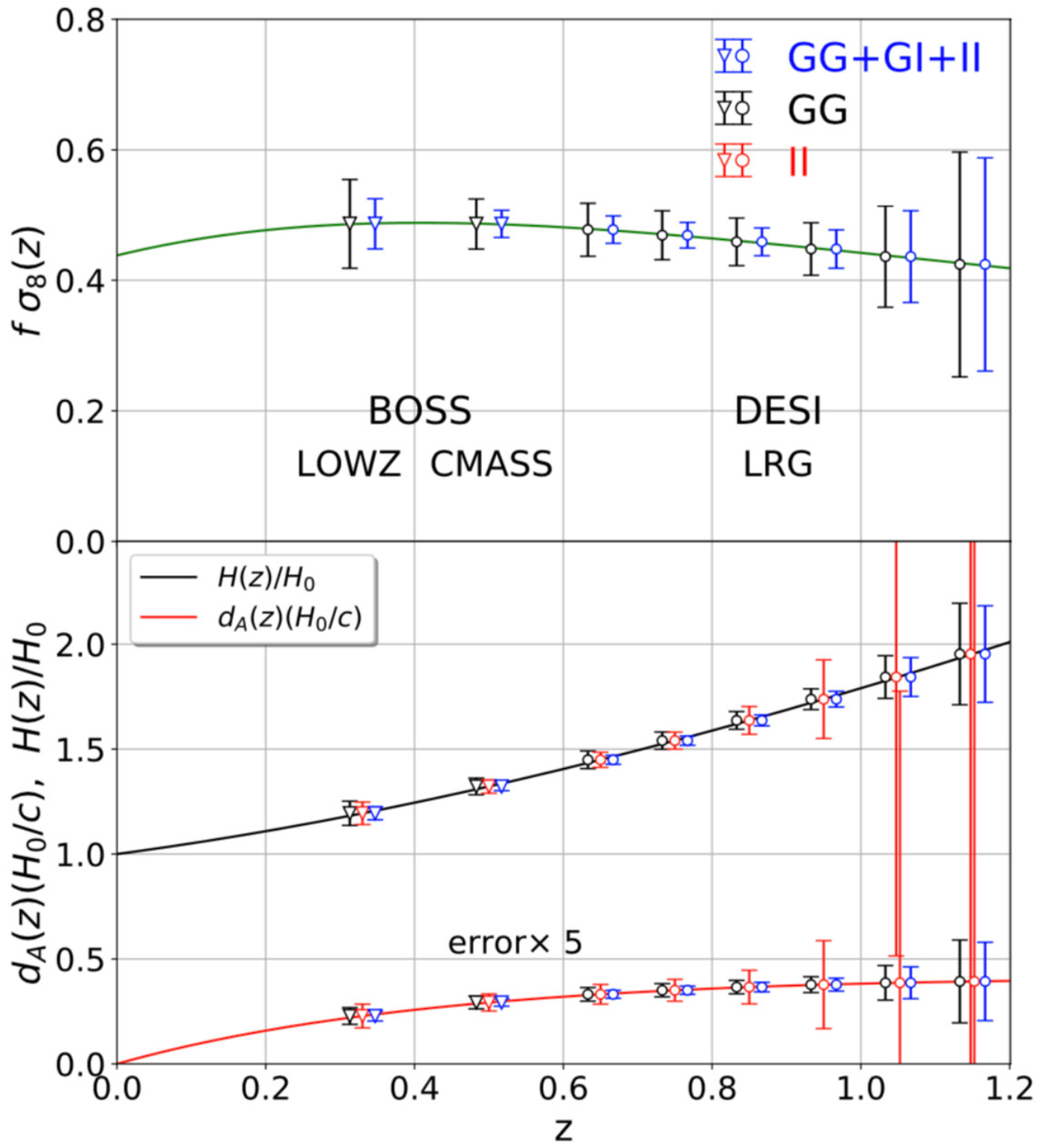

Taruya & Okumura 2020

INTRINSIC ALIGNMENT – PROBE OF COSMOLOGY

- Complementary probe of Baryonic Acoustic Oscillation, Redshift Space Distortion (Chisari+2013, Taruya & Okumura2020)
- Special probe of anisotropic Primordial non-Gaussianity

Akitsu+2020

IA –> sensitive probe of anisotropic PNG (s=2)

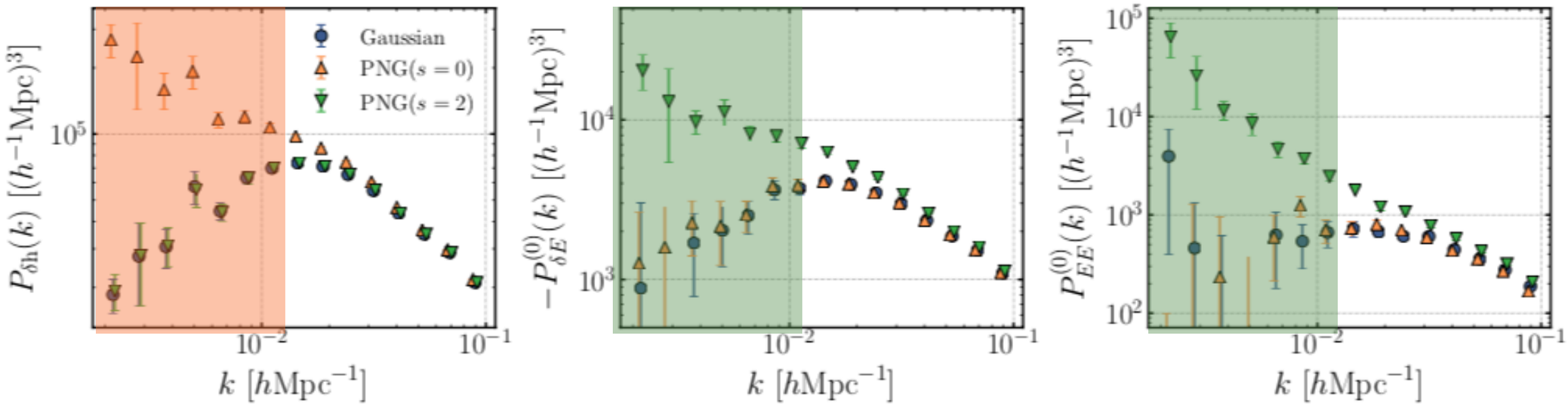

Clustering –> isotropic PNG (s=0)

Dalal+2008

$$B_\Phi(\mathbf{k}_1,\mathbf{k}_2,\mathbf{k}_3) = 2\sum_{\ell=0,1,2,\cdots} f_{\rm NL}^{s=\ell}\left[\mathcal{L}_\ell(\hat{\mathbf{k}}_1\cdot\hat{\mathbf{k}}_2)P_\phi(k_1)P_\phi(k_2) + 2\ \text{perms.}\right]$$

EMISSION LINE GALAXY (ELG) SURVEYS

Prime Focus Spectrograph

SuMIRe

	Testing ΛCDM	Assembly history of galaxies	Importance of IGM
CO	• Nature & role of neutrinos • Expansion rate via BAO up to z=2.4 • PFS+HSC tests of GR • Curvature of space: Ω_K • Primordial power spectrum	• PFS+HSC synergy • Absorption probes with PFS/SDSS QSOs around PFS/HSC host galaxies	• Search for emission from stacked spectra
GA	• Nature of DM (dSphs) • Structure of MW dark halo	• Stellar kinematics and chemical abundances – MW & M31 assembly history	• dSph as relic probe of reionization feedback • Past massive star IMF from element abundances
GE	• Small-scale tests of structure growth	• Halo-galaxy connection: $M_*/M_{\rm halo}$ • Outflows & inflows of gas • Environment-dependent evolution	• Physics of cosmic reionization via LAEs & 21cm studies • Tomography of gas & DM

PFS survey cosmology: use single tracer ([OII] emission line galaxies, i.e. ELGs) to map evolution of the large-scale structure of the Universe in a wide range of redshifts, $0.6 < z < 2.4$, over 1400 deg^2 sky area covered also by the HSC image survey

DESI targets:

Galaxy type	Redshift range	Bands used	Targets per deg^2	Exposures per deg^2	Good z's per deg^2	Baseline sample
LRG	0.4–1.0	r,z,$W1$	350	580	285	4.0 M
ELG	0.6–1.6	g,r,z	2400	1870	1220	17.1 M
QSO (tracers)	< 2.1	g,r,z,$W1$,$W2$	170	170	120	1.7 M
QSO (Ly-α)	> 2.1	g,r,z,$W1$,$W2$	90	250	50	0.7 M
Total in dark time			**3010**	**2870**	**1675**	**23.6 M**
BGS	0.05–0.4	r	700	700	700	9.8 M
Total in bright time			**700**	**700**	**700**	**9.8 M**

DESI Collaboration, 2016

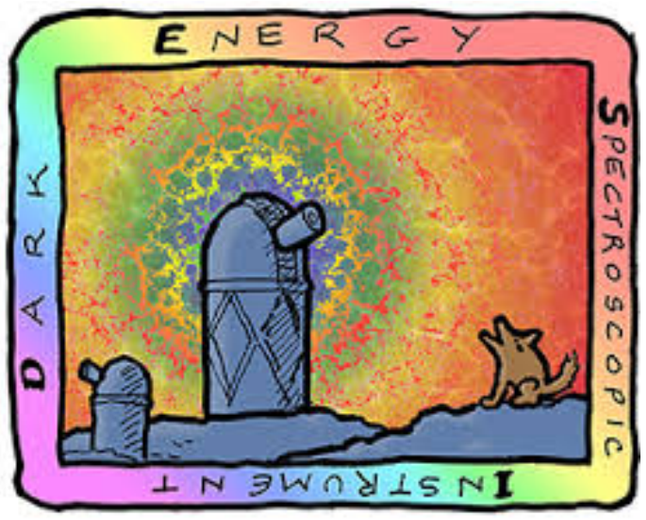

INTRINSIC ALIGNMENT OF ELGS

Mandelbaum+2011, Yao+2020

Blue star-forming galaxies – no clear IA signal detected so far

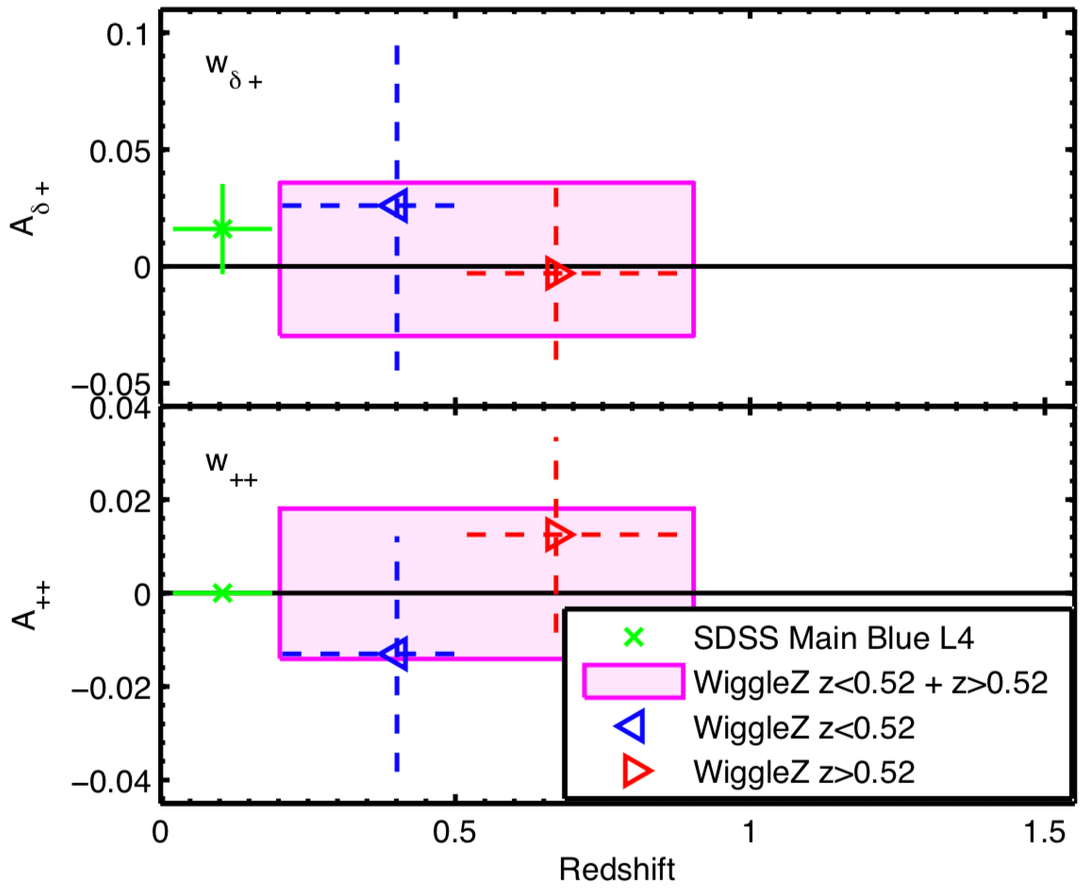

OBSERVATION

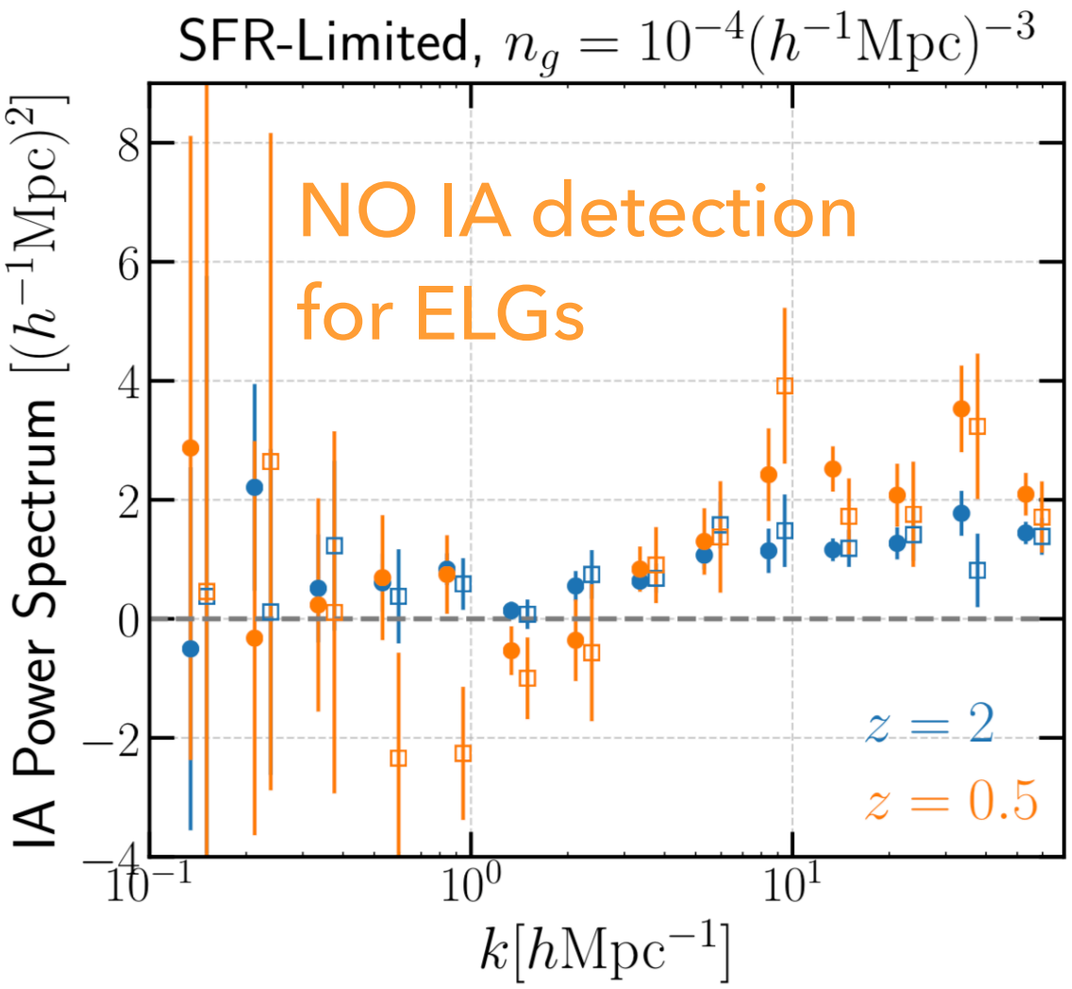

Shi+2021a

SIMULATION

INTRINSIC ALIGNMENT OF ELGS

Mandelbaum+2011, Yao+2020

Blue star-forming galaxies – no clear IA signal detected so far

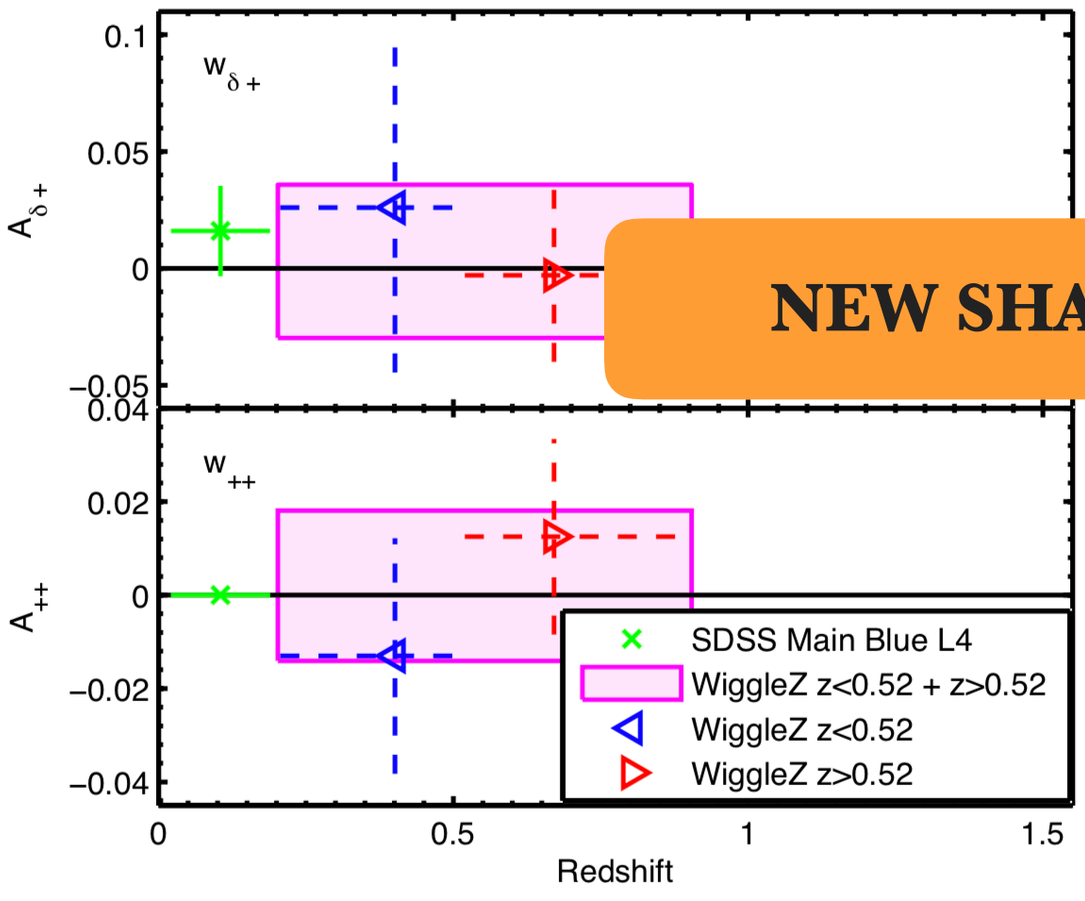

NEW SHAPE ESTIMATOR

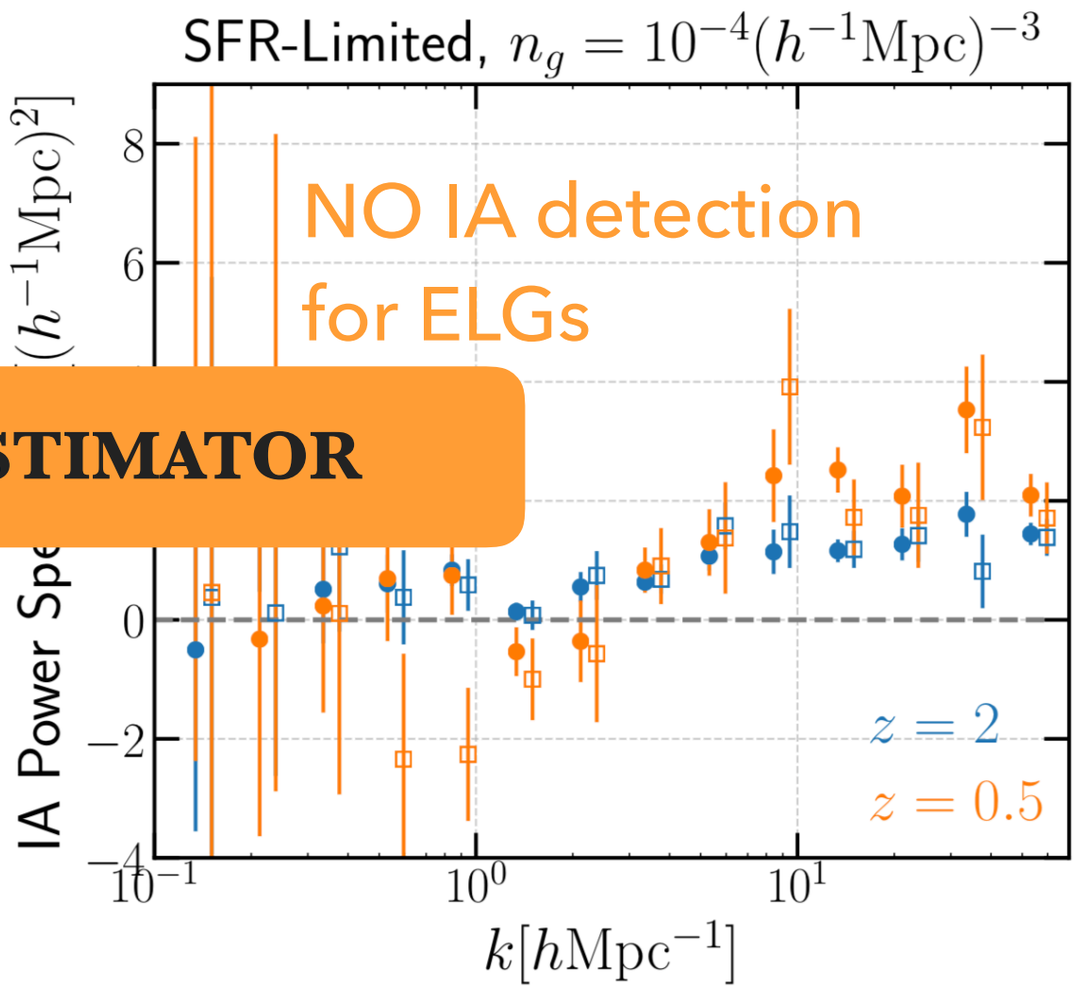

Shi+2021a

OBSERVATION

SIMULATION

SHAPE ESTIMATOR

OBSERVATION

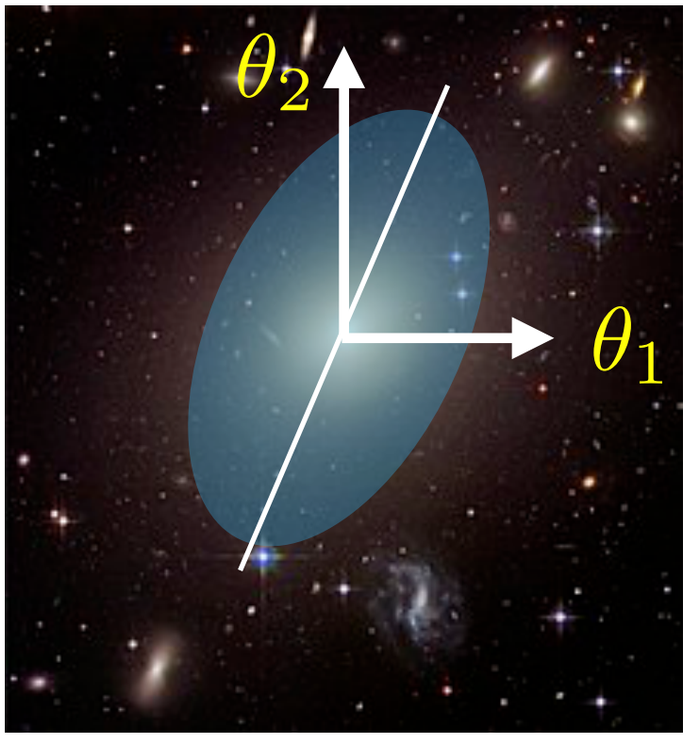

$$I_{ij} = \frac{\int d^2\theta w(\theta) f(\theta) \theta_i \theta_j}{\int d^2\theta w(\theta) f(\theta)}$$

Taruya san's talk

SIMULATION

$$I_{ij}^{\rm reduced} = \frac{\sum_n m_n \frac{x_{ni} x_{nj}}{r_n^2}}{\sum_n m_n}$$

See Kurita+2020 for tests of
various shape estimators in simulations

SELECTION OF ELGS IN TNG300

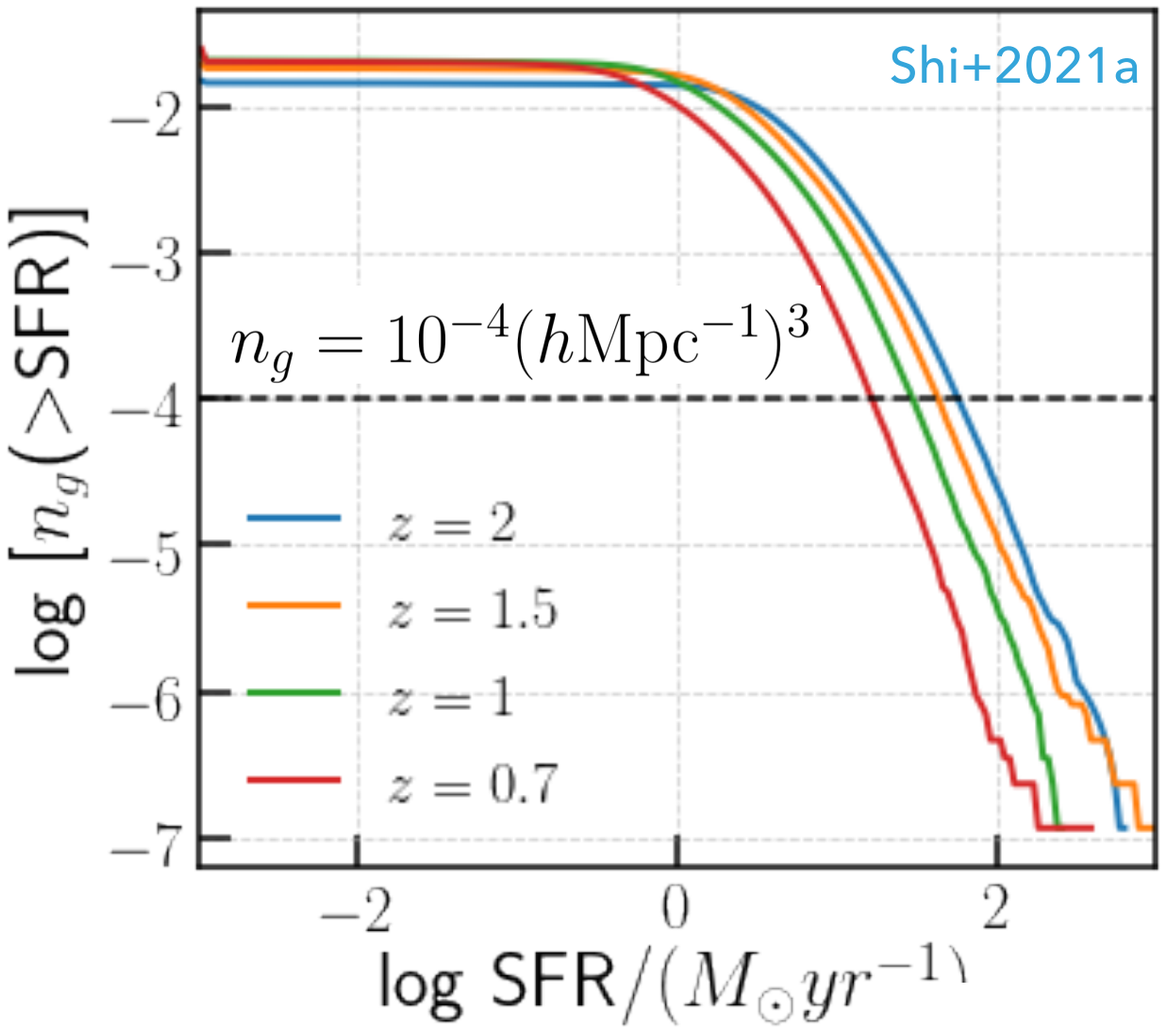

SFR ranked selected galaxies

roughly corresponds to

[OII] emission line strength selected galaxies

Gonzalez-Perez+2020; Osato & Okumura 2021, in prep

Table 1
Properties of ELGs in Illustris-TNG300, Studied in this Work

z	$\langle \log M_\star \rangle$	$\langle \log M_{\mathrm{halo}} \rangle$	$\langle \mathrm{SFR} \rangle$	f_{cen}	A_{IA}	σ_ϵ
0.5	10.39	13.20	25.75	0.667	15.39 ± 2.96	0.43
1.0	10.41	13.04	47.78	0.682	15.26 ± 2.89	0.41
1.5	10.42	12.88	71.64	0.741	12.86 ± 2.83	0.39
2.0	10.41	12.67	94.01	0.798	15.45 ± 2.84	0.40

Shi+2021b

Ray-tracing simulation using Pégase.3 code

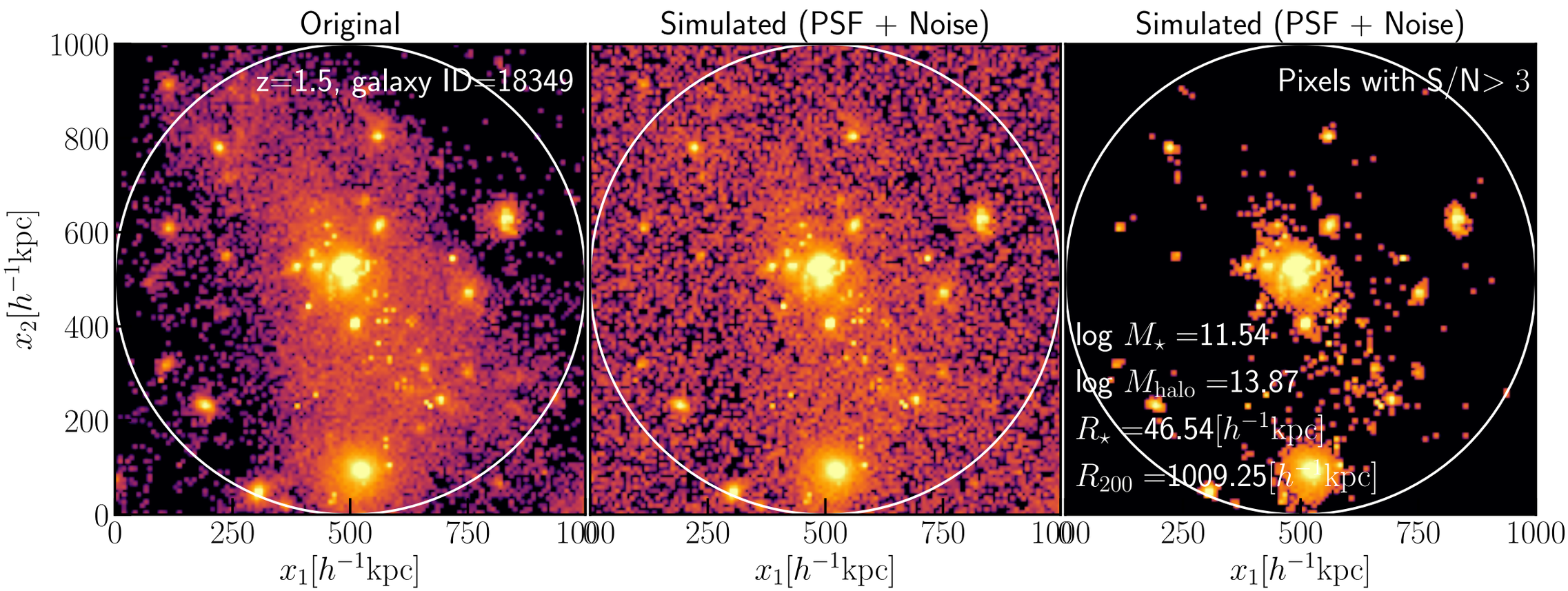

0.6 arcsec seeing
1200sec exposure
8.2m Subaru aperture

Shi+2021b

APERTURE SHAPE ESTIMATOR

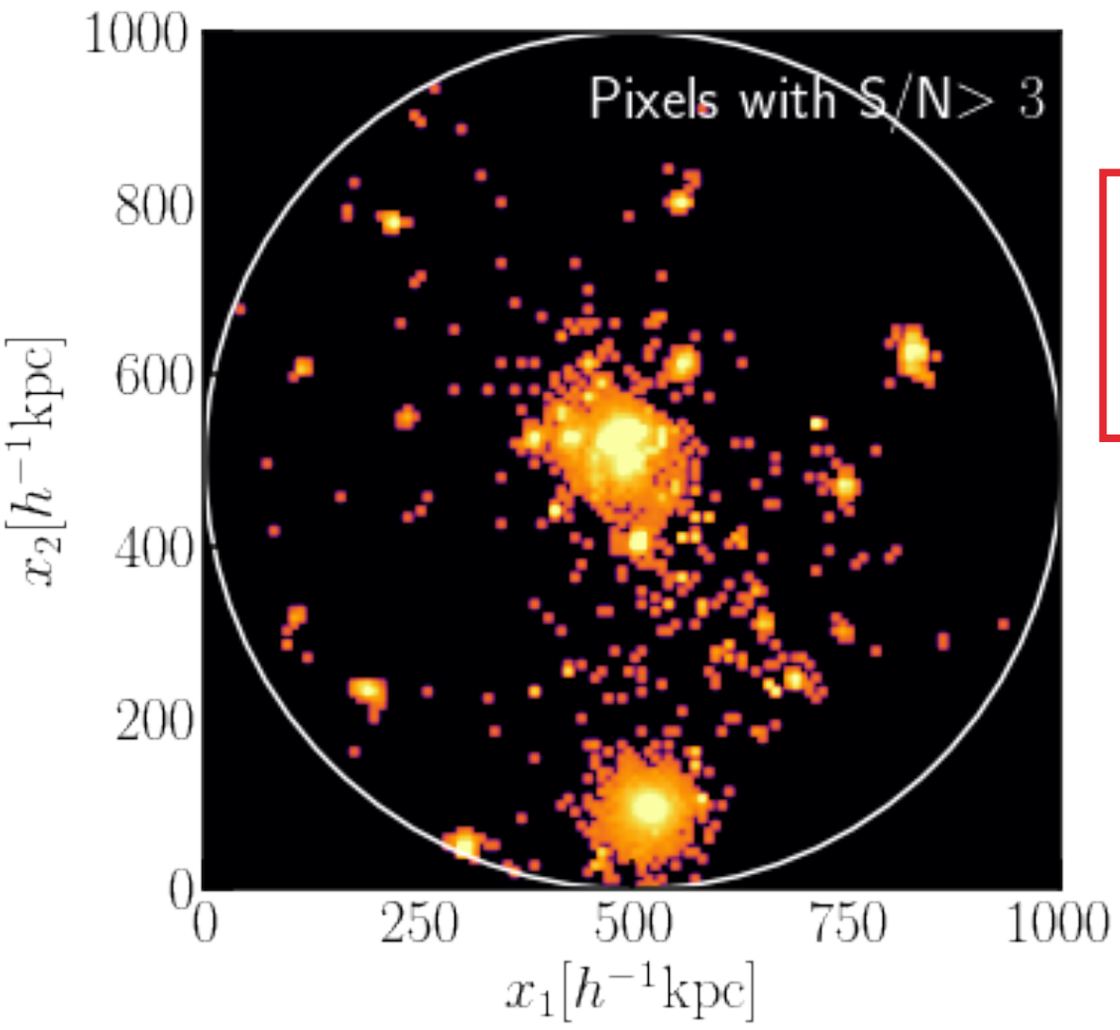

Shi+2021b

$$I_{ij}^{\mathrm{ap}} = \frac{\sum_{n;(S/N)_{\mathrm{pix}}>3;r_n^{\mathrm{2D}}\leq 500h^{-1}\mathrm{kpc}} f_n x_{ni} x_{nj}}{\sum_{n;(S/N)_{\mathrm{pix}}>3;r_n^{\mathrm{2D}}\leq 500h^{-1}\mathrm{kpc}} f_n}$$

f_n —— flux of pixels

x_{ni}, x_{nj} —— distance of pixels to the ELG

1Mpc/h aperture *versus* **within ELG**

no weighting *versus* **1/r² weighting**

Reduced inertia tensor

$$I_{ij}^{\mathrm{reduced}} = \frac{\sum_n m_n \frac{x_{ni}x_{nj}}{r_n^2}}{\sum_n m_n}$$

m_n —— mass of the stellar particles within the galaxy

APERTURE SHAPE ESTIMATOR

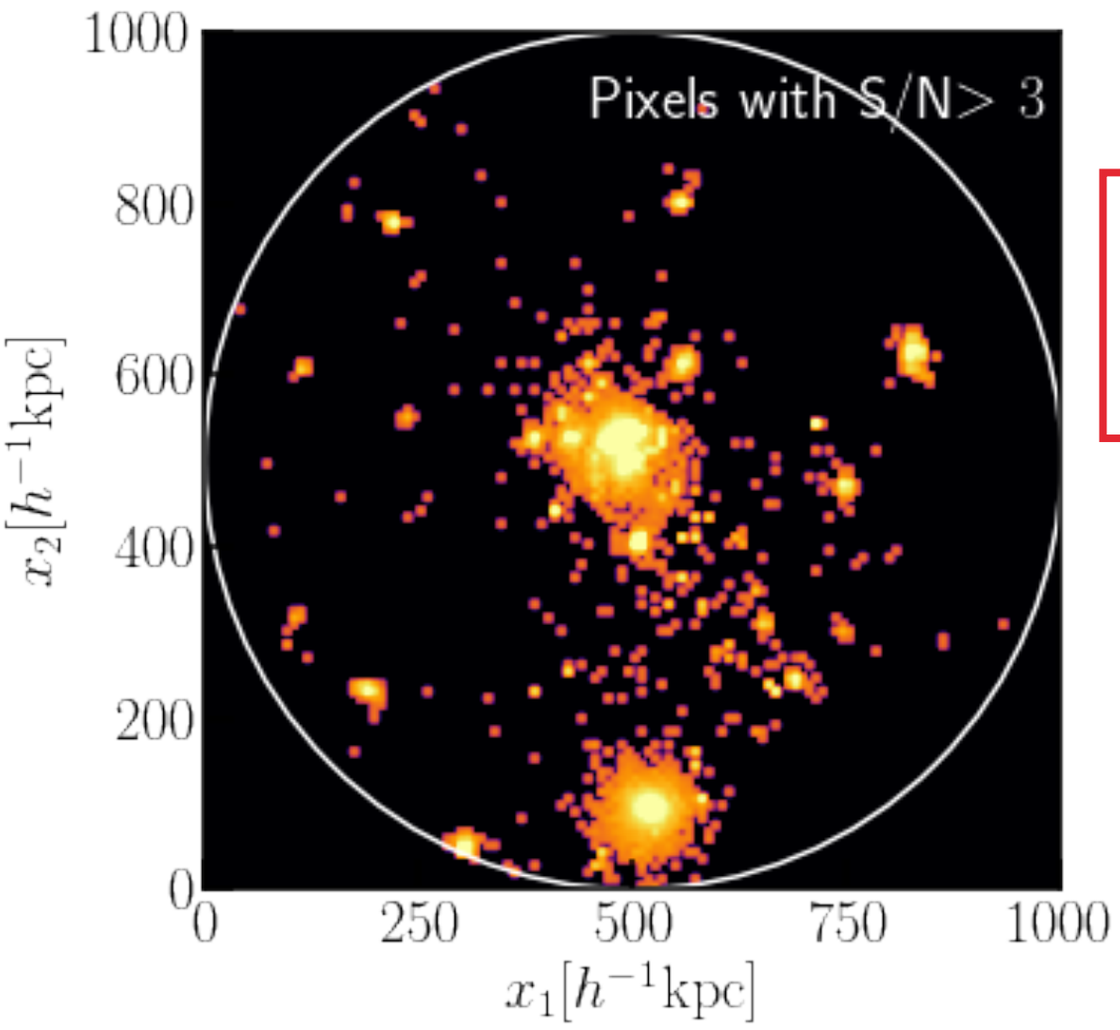

Shi+2021b

$$I_{ij}^{\mathrm{ap}} = \frac{\sum_{n;(S/N)_{\mathrm{pix}}>3;r_n^{\mathrm{2D}}\leq 500h^{-1}\mathrm{kpc}} f_n x_{ni} x_{nj}}{\sum_{n;(S/N)_{\mathrm{pix}}>3;r_n^{\mathrm{2D}}\leq 500h^{-1}\mathrm{kpc}} f_n}$$

f_n —— flux of pixels

x_{ni}, x_{nj} —— distance of pixels to the ELG

$$\epsilon_1 \equiv \frac{I_{11}-I_{22}}{I_{11}+I_{22}}, \epsilon_2 \equiv \frac{2I_{12}}{I_{11}+I_{22}}$$

Reduced inertia tensor

$$I_{ij}^{\mathrm{reduced}} = \frac{\sum_n m_n \frac{x_{ni}x_{nj}}{r_n^2}}{\sum_n m_n}$$

m_n —— mass of the stellar particles within the galaxy

INTRINSIC ALIGNMENT OF ELGS

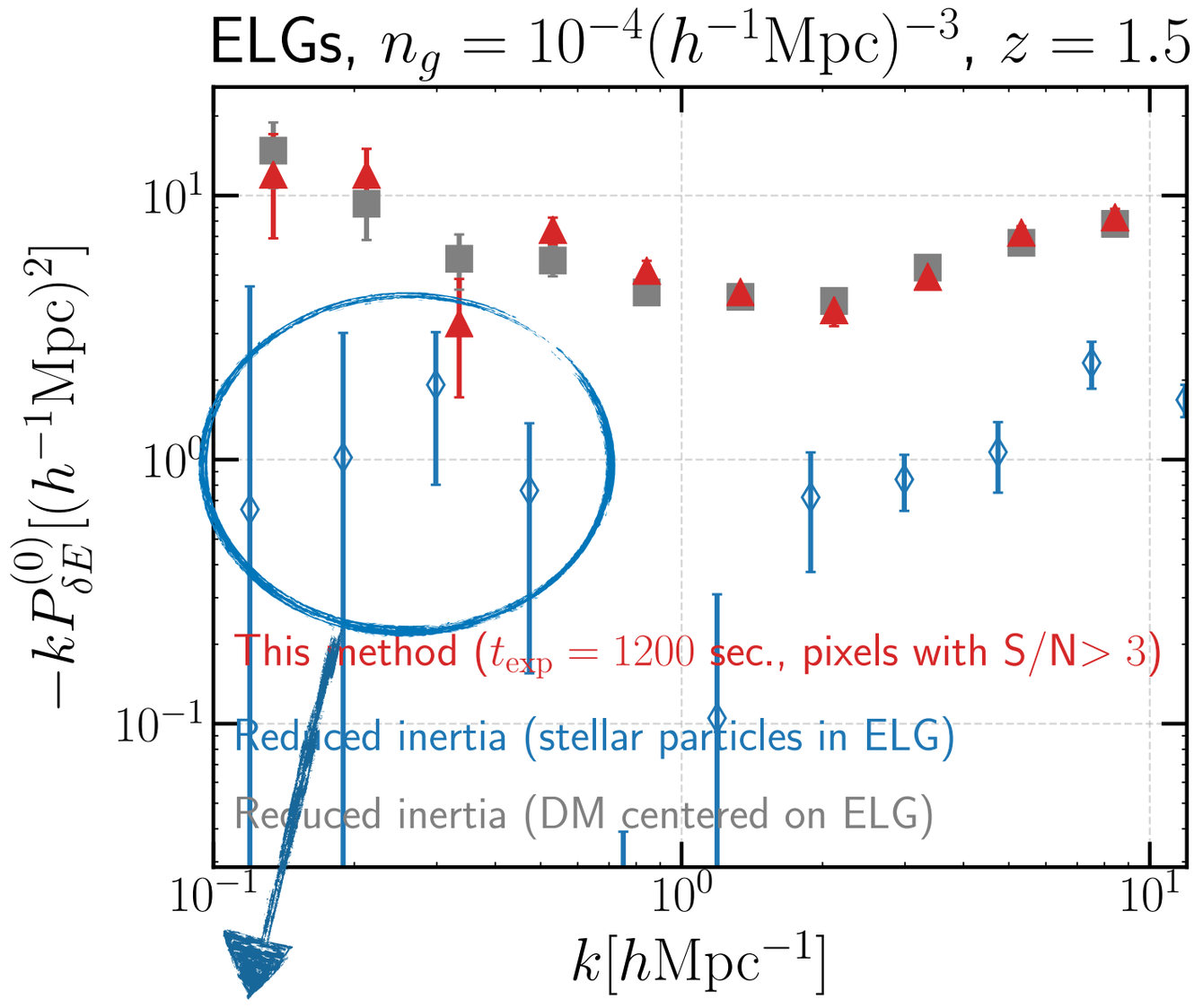

Shi+2021b

High S/N IA signal obtained with

Aperture shape estimator

No IA signal with reduced shape estimator

$$\langle \gamma_E(\boldsymbol{k})\delta_m(\boldsymbol{k'})\rangle \equiv (2\pi)^3\delta_D(\boldsymbol{k}+\boldsymbol{k'})P_{\delta E}(\boldsymbol{k})$$

→ IA power spectrum

(Kurita+2020, Shi+2021a)

Shi+2021b

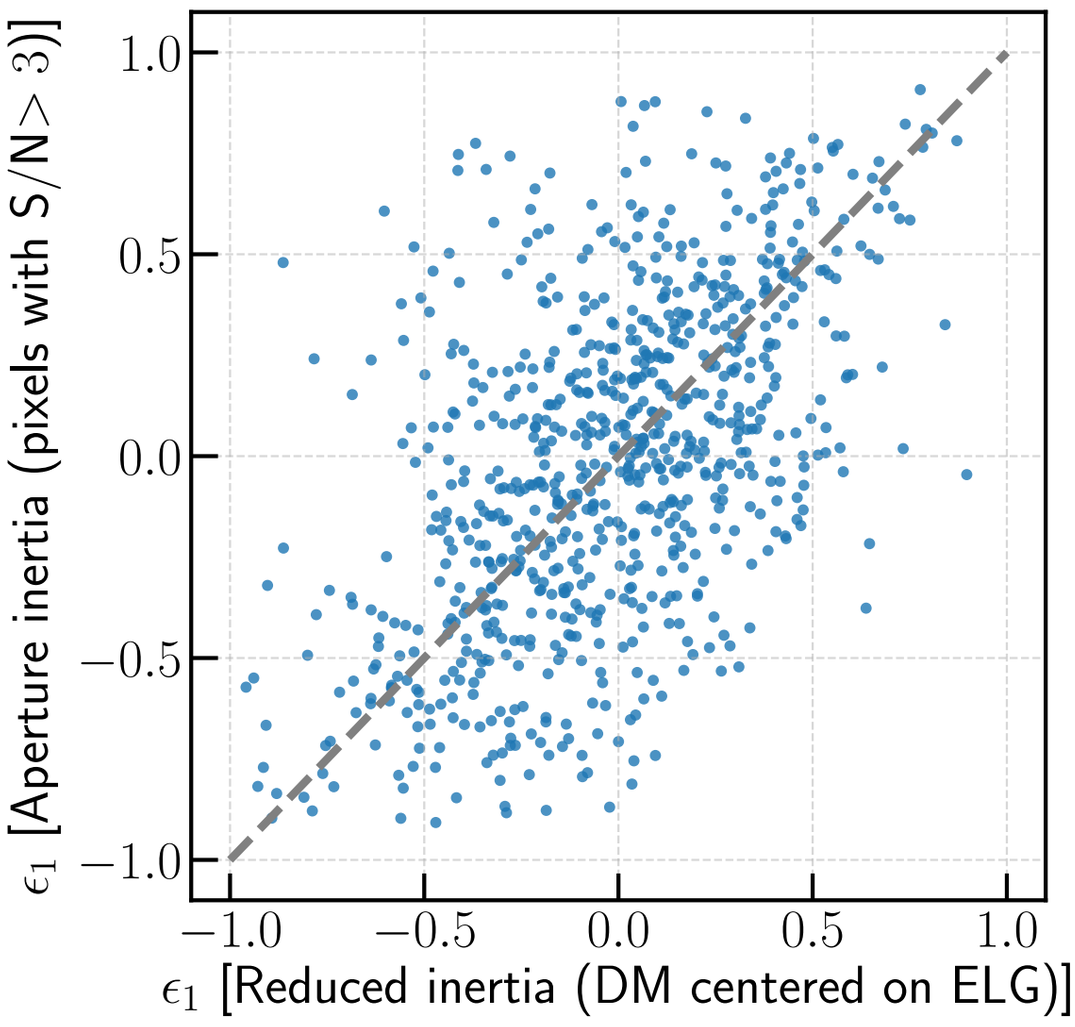
ϵ_1 [Aperture inertia (pixels with S/N> 3)]
ϵ_1 [Reduced inertia (DM centered on ELG)]
1.0
0.5
0.0
−0.5
−1.0
−1.0
−0.5
0.0
0.5
1.0

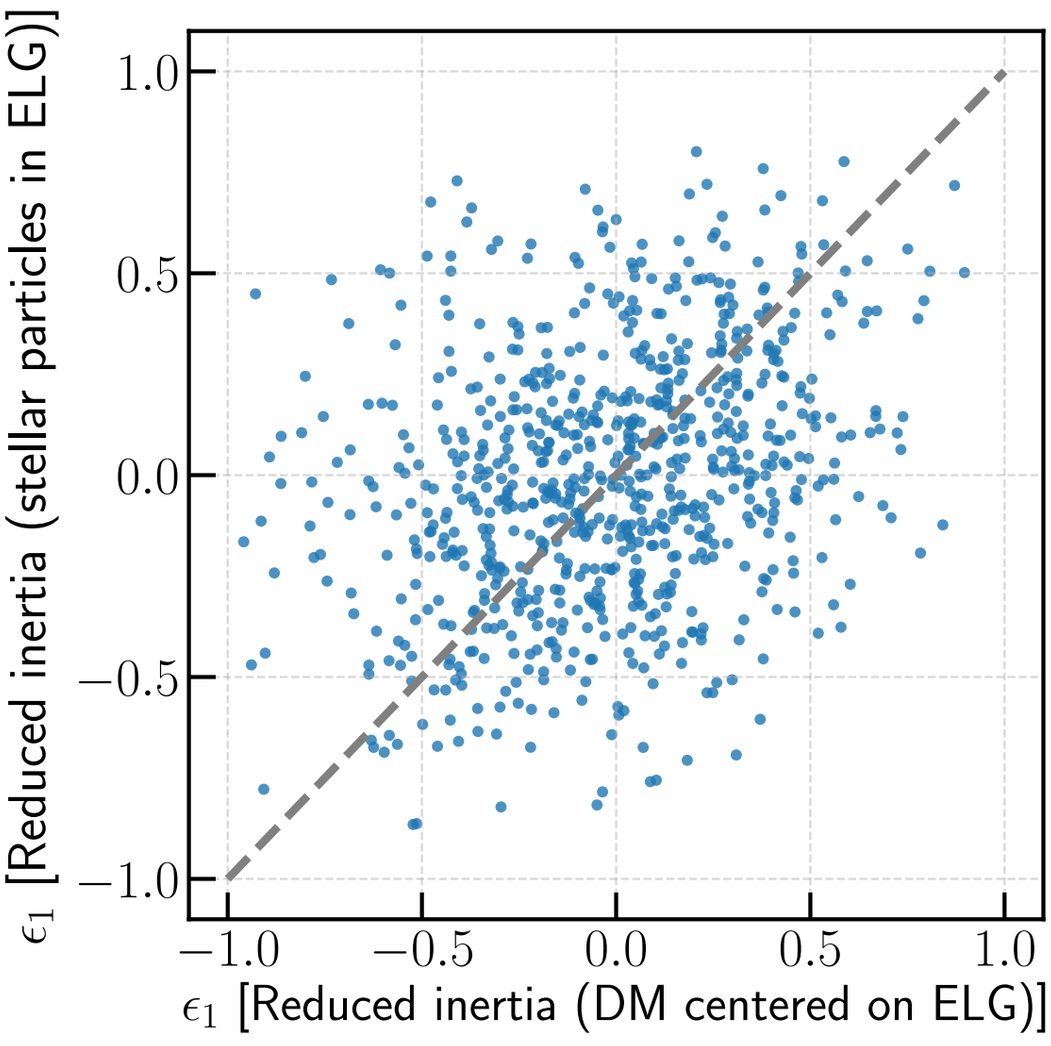
ϵ_1 [Reduced inertia (stellar particles in ELG)]
ϵ_1 [Reduced inertia (DM centered on ELG)]
1.0
0.5
0.0
−0.5
−1.0
−1.0
−0.5
0.0
0.5
1.0

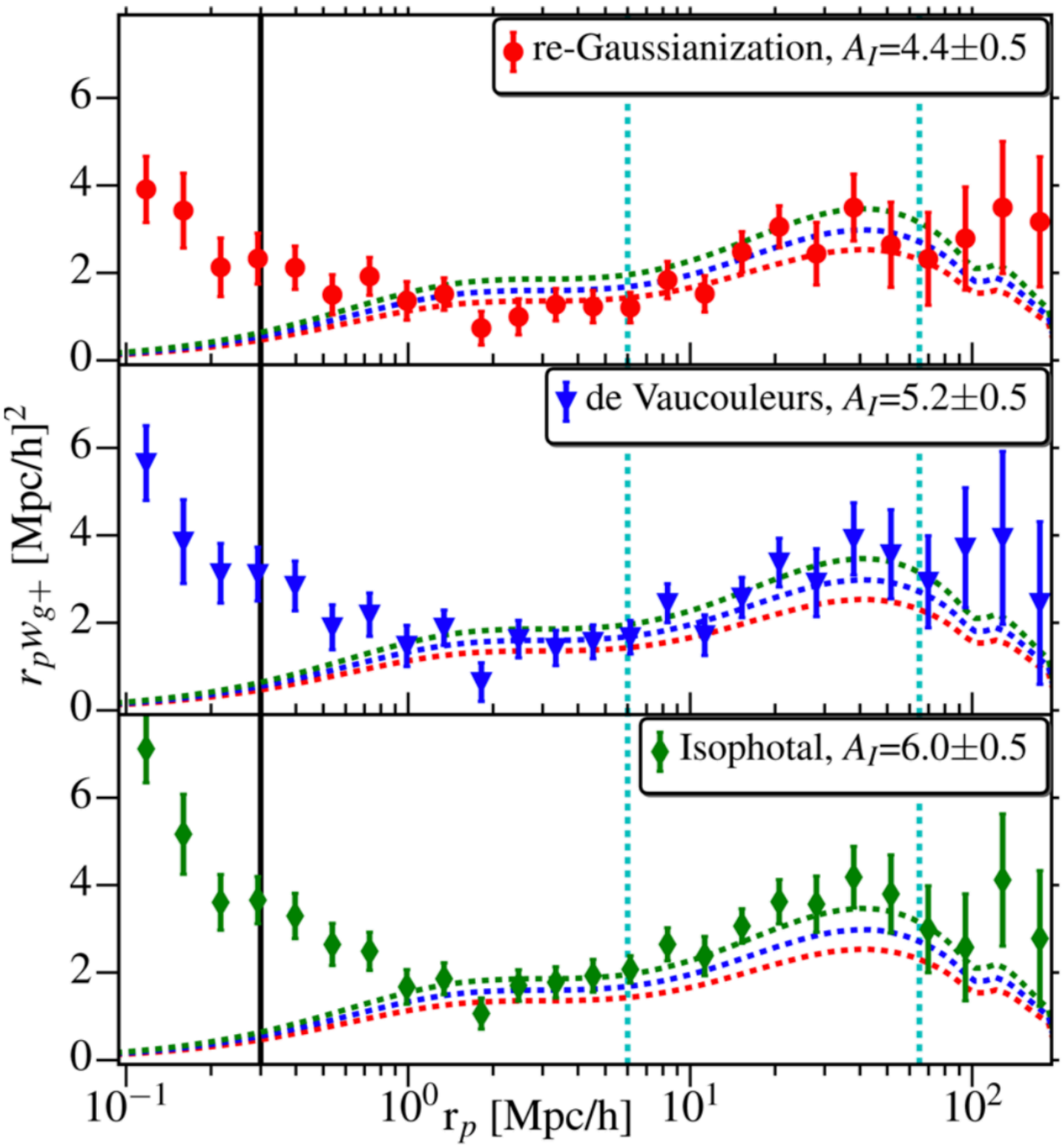

Singh+2015b

Outer region of luminous reds galaxies are more responsive to tidal field

APERTURE SHAPE ESTIMATOR - APPLICATION TO LRGS

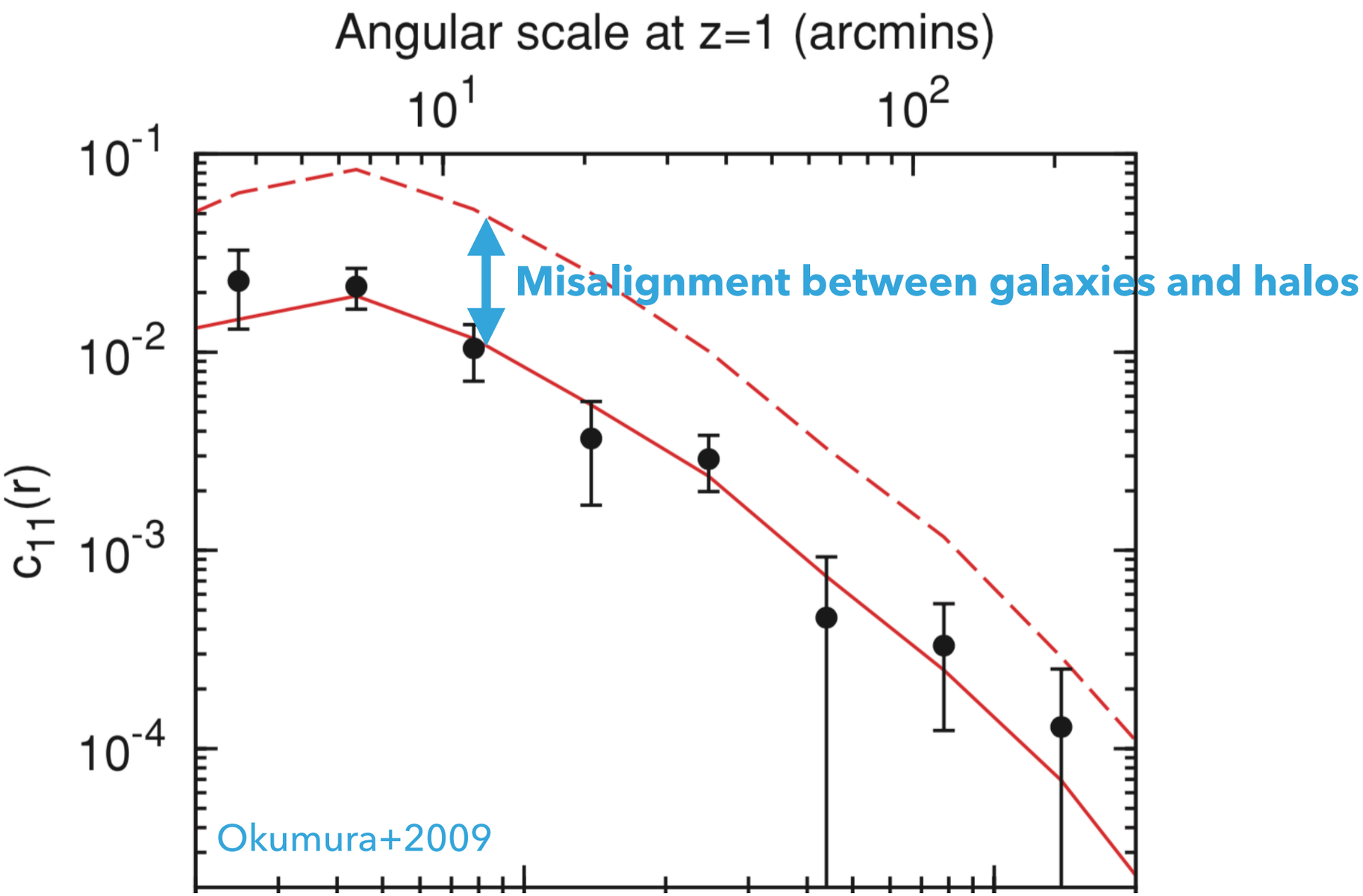

SUMMARY AND WORKING DIRECTION

Galaxy intrinsic alignment contaminates weak lensing cosmology

- 3D IA power spectrum — full 2pt correlation information, scale dependence, high S/N ratio
- Mass, redshift, scale, morphological, environmental dependence of both shape and spin are studied in the simulation - useful for constraining the galaxy formation physics by comparing to observations
- Work in progress — direct measure intrinsic alignment in HSC survey for LRGs

Galaxy intrinsic alignment as cosmological probe

- The cosmological information encoded in IA signal of galaxies targeted by ongoing/future surveys can be promisingly extracted with our aperture shape estimator
- Work in progress — apply this estimator to observed image

TATT

Blazek+2019

$$\gamma_{ij}^{I} = \underbrace{C_1 s_{ij}}_{\text{Tidal Alignment}} + \underbrace{C_{1\delta}(\delta \times s_{ij})}_{\text{Density Weighting}} + \underbrace{C_2 \left[\sum_{k=0}^{2} s_{ik} s_{kj} - \frac{1}{3} \delta_{ij} s^2 \right]}_{\text{Tidal Torquing}} + \ldots ,$$

$$C_1 = -A_1 \bar{C}_1 \frac{\Omega_{\rm m} \rho_{\rm crit}}{D(z)},$$

$$C_2 = 5 A_2 \bar{C}_1 \frac{\Omega_{\rm m} \rho_{\rm crit}}{D^2(z)}.$$

$$C_{1\delta} = -A_{1\delta} \bar{C}_1 \frac{\Omega_{\rm m} \rho_{\rm crit}}{D(z)},$$

Samuroff+2020

Model	Parameter	Prior
NLA	A_1	$\mathrm{U}[-6, 6]$
	b_g	$\mathrm{U}[0.05, 8]$
TATT	A_1	$\mathrm{U}[-6, 6]$
	A_2	$\mathrm{U}[-6, 6]$
	$b_{\rm TA}$	$\mathrm{U}[-6, 6]$
	b_g	$\mathrm{U}[0.05, 8]$

optical imaging surveys

HSC (UD)
LSST (deep)
SXDS
HSC (deep)
DES (SN-deep)
COSMOS
LSST (wide)
CFHTLS (deep)
HSC (wide)
PS1 (MDS)
NDWFS
DES (SN-shallow)
CFHTLS (wide)
KiDS
DES (wide)
Euclid
PS2
BCS
Stripe82
RCS2
PS1 (3π)
VST-ATLAS
SkyMapper
SDSS

future
ongoing
completed

r_{lim} (AB, 5σ, 2" aperture)

28
27
26
25
24
23

1
10^1
10^2
10^3
10^4

Area [deg²]

INTRINSIC ALIGNMENT – OBSERVATIONS

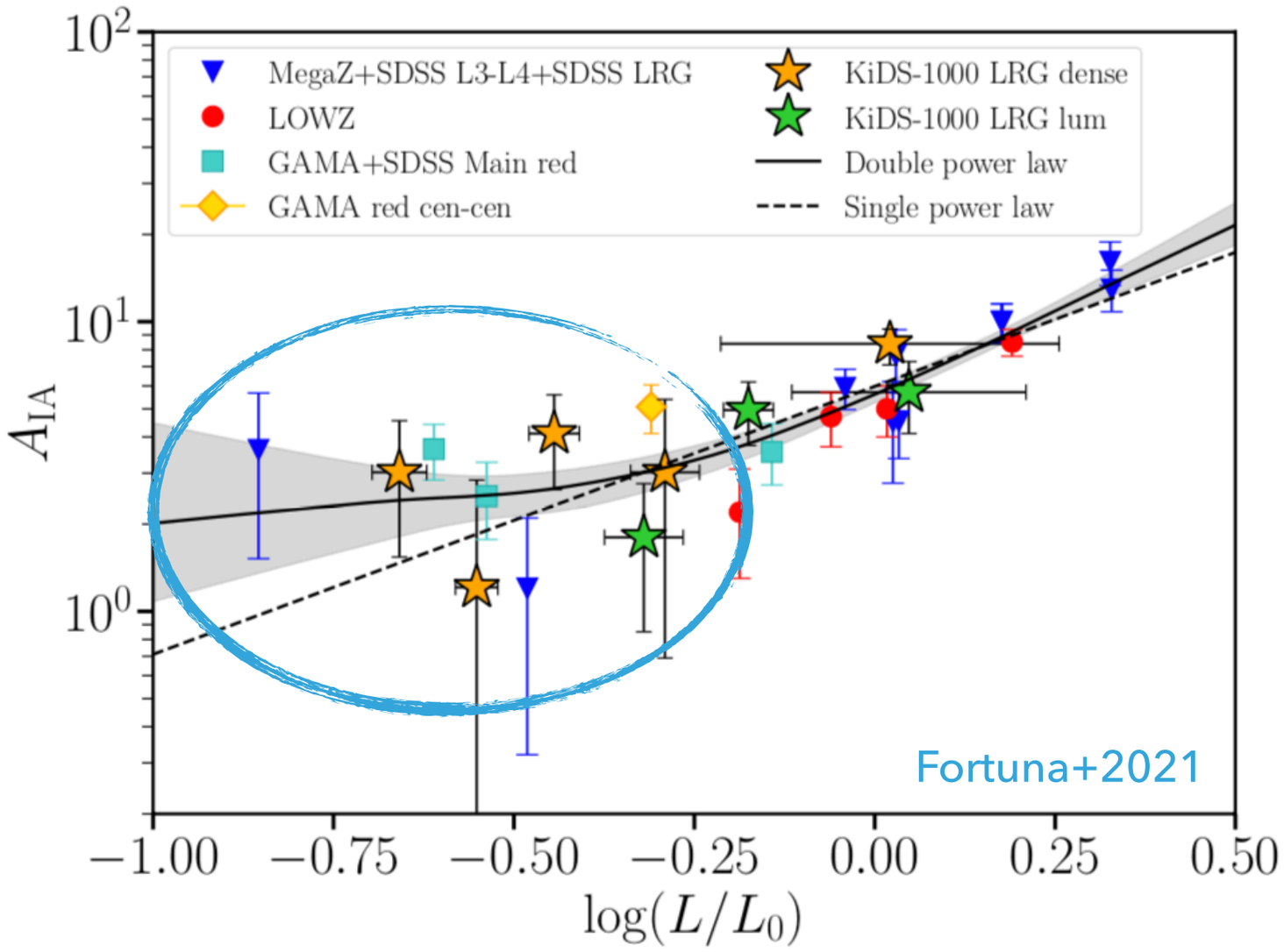

INTRINSIC ALIGNMENT – MASS AND Z DEPENDENCE

Kurita+2020

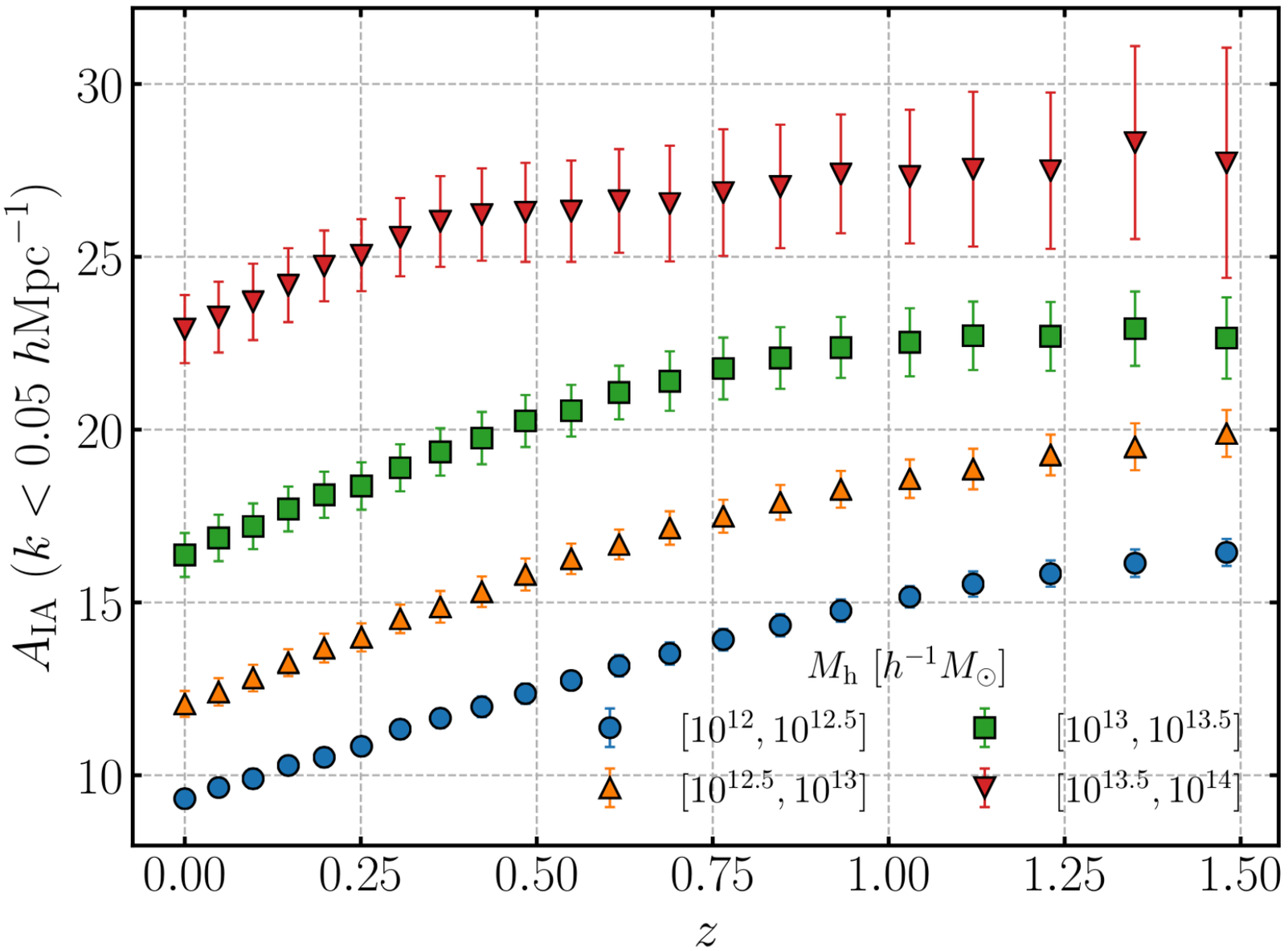

Shi+2021b

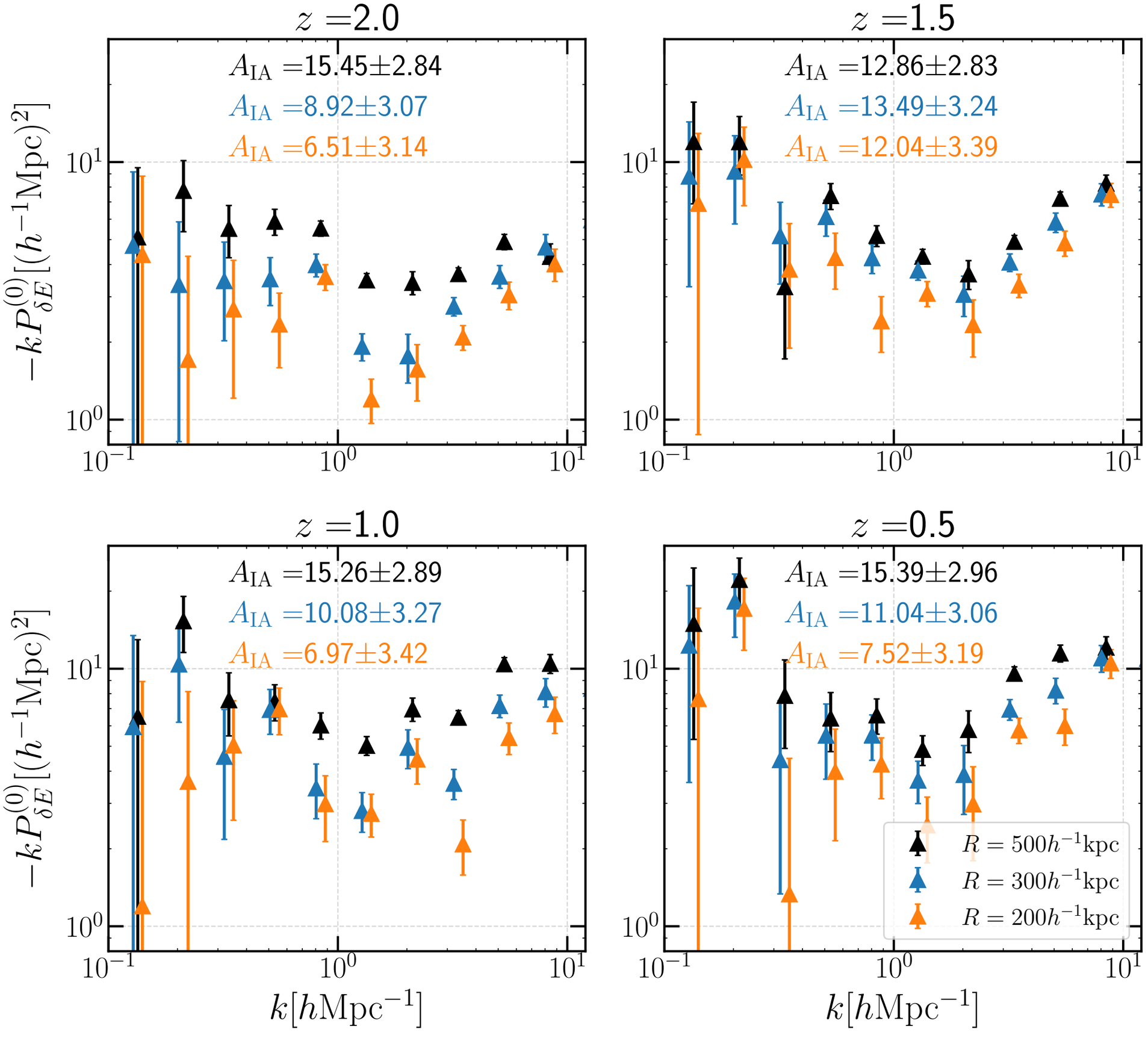
z =2.0
$A_{\rm IA}$ =15.45±2.84
$A_{\rm IA}$ =8.92±3.07
$A_{\rm IA}$ =6.51±3.14
z =1.5
$A_{\rm IA}$ =12.86±2.83
$A_{\rm IA}$ =13.49±3.24
$A_{\rm IA}$ =12.04±3.39
z =1.0
$A_{\rm IA}$ =15.26±2.89
$A_{\rm IA}$ =10.08±3.27
$A_{\rm IA}$ =6.97±3.42
z =0.5
$A_{\rm IA}$ =15.39±2.96
$A_{\rm IA}$ =11.04±3.06
$A_{\rm IA}$ =7.52±3.19
$R = 500h^{-1}$kpc
$R = 300h^{-1}$kpc
$R = 200h^{-1}$kpc
$-kP^{(0)}_{\delta E}[(h^{-1}{\rm Mpc})^2]$
$k[h{\rm Mpc}^{-1}]$

Shi+2021b

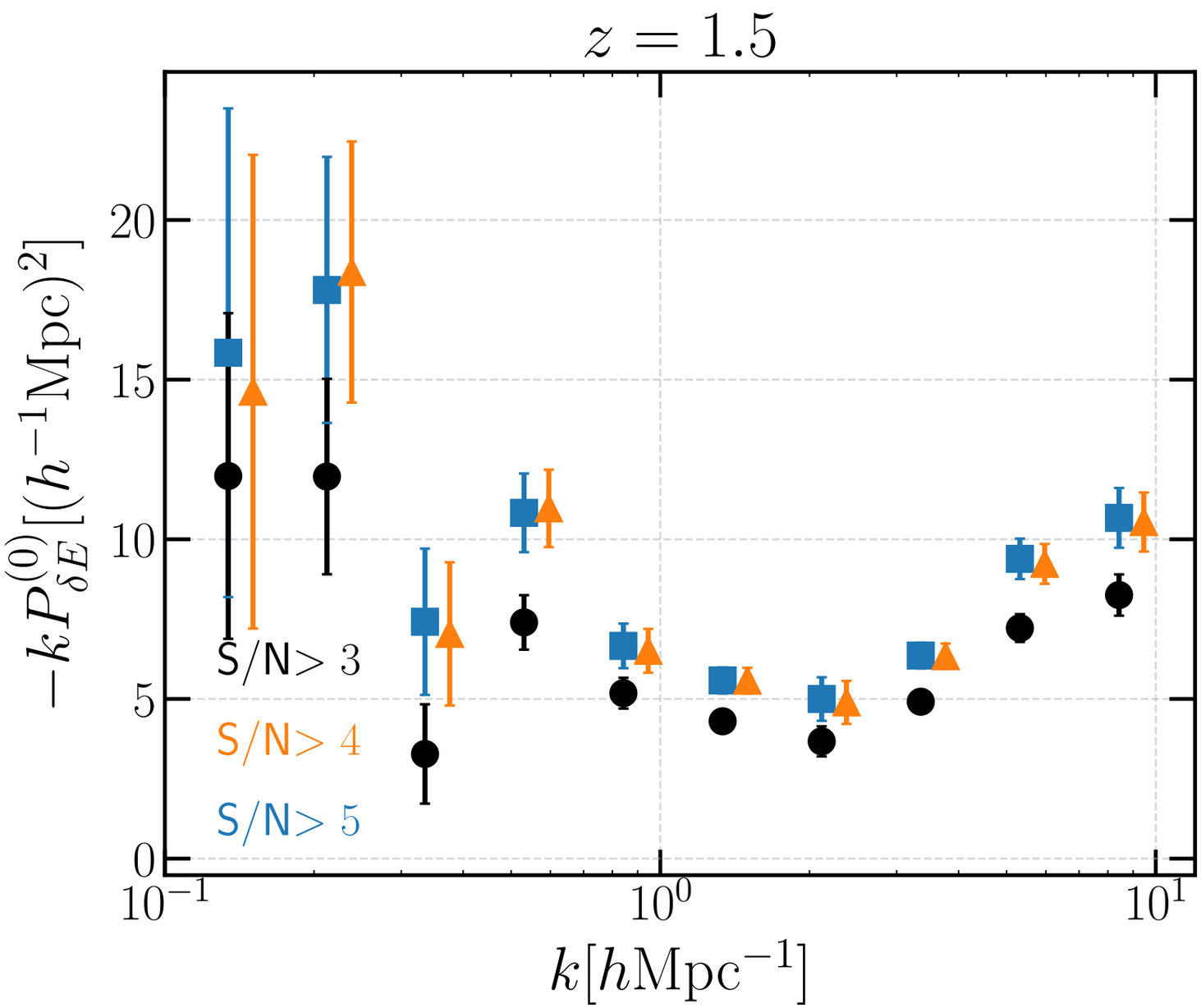
$z = 1.5$
$-kP_{\delta E}^{(0)}[(h^{-1}\mathrm{Mpc})^2]$
20
15
10
5
0
S/N> 3
S/N> 4
S/N> 5
10^{-1}
10^{0}
10^{1}
$k[h\mathrm{Mpc}^{-1}]$

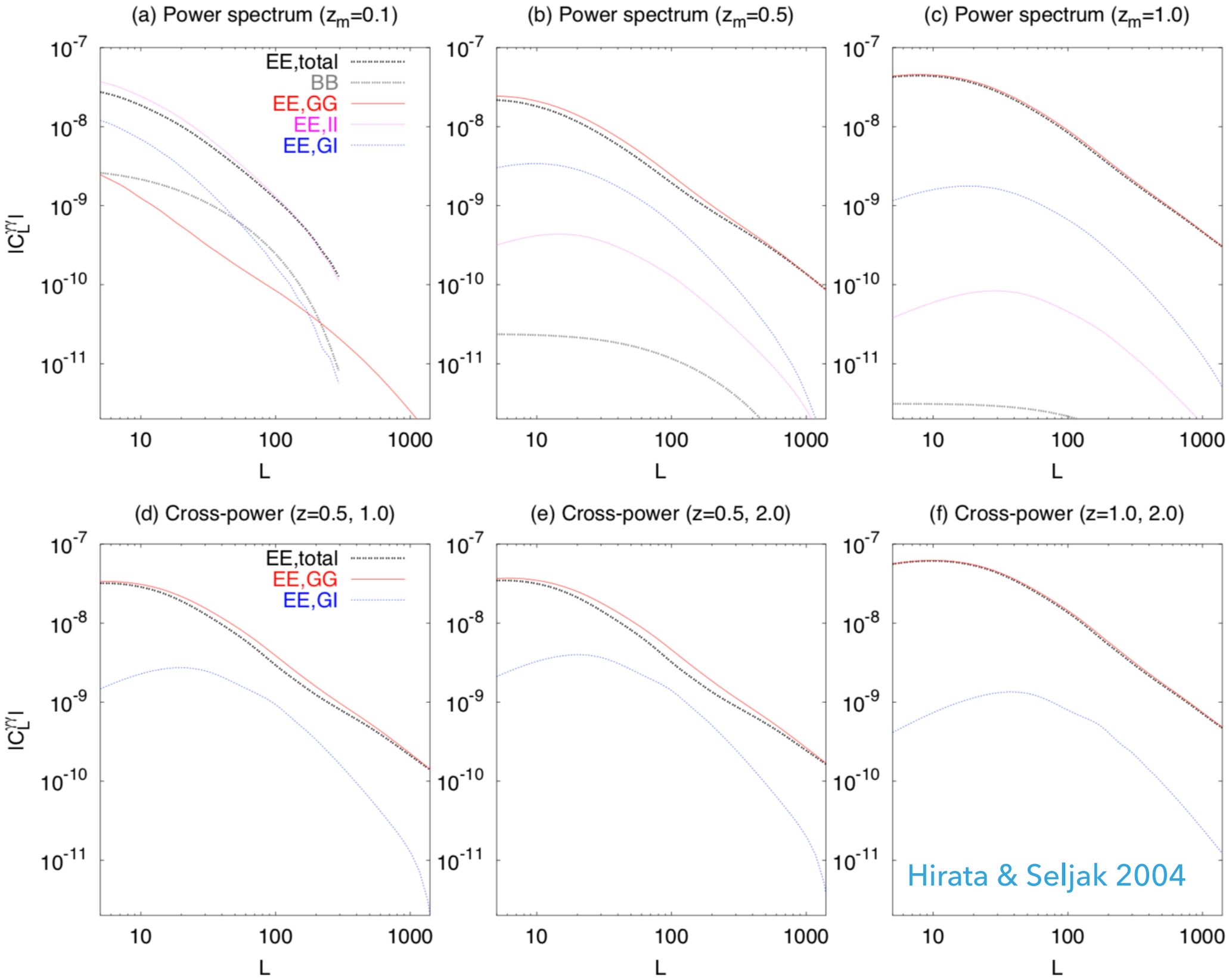
(a) Power spectrum (z_m=0.1)
(b) Power spectrum (z_m=0.5)
(c) Power spectrum (z_m=1.0)
EE,total
BB
EE,GG
EE,II
EE,GI
$IC_L^{\gamma\gamma}I$
L
(d) Cross-power (z=0.5, 1.0)
(e) Cross-power (z=0.5, 2.0)
(f) Cross-power (z=1.0, 2.0)
Hirata & Seljak 2004